International Journal of Applied Metaheuristic Computing
Volume 13 • Issue 1

Alternated Superior Chaotic Biogeography-Based Algorithm for Optimization Problems

Deepak Kumar, Central University of Rajasthan, India*
https://orcid.org/0000-0001-6826-4473

Mamta Rani, Central University of Rajasthan, India

ABSTRACT

In this study, the authors consider a switching strategy that yields a stable desirable dynamic behaviour when it is applied alternatively between two undesirable dynamical systems. Over the last few years, dynamical systems employed "$\text{chaos}_1 + \text{chaos}_2 = \text{order}$" and "$\text{order}_1 + \text{order}_2 = \text{chaos}$" (vice-versa) to control and anti control of chaotic situations respectively. To find parameter values for these kinds of alternating situations, comparison is being made between bifurcation diagrams of a map and its alternate version, which, on their own, means independent of one another, yield chaotic orbits. However, the parameter values yield a stable periodic orbit, when alternating strategy is employed upon them. It is interesting to note that we look for stabilization of chaotic trajectories in nonlinear dynamics, with the assumption that such chaotic behaviour is not desirable for a particular situation. The method described in this paper is based on the Parrondo's paradox, where two losing games can be alternated, yielding a winning game, in a superior orbit.

KEYWORDS

Alternated Logistic Map, ASCBBO, BBO, CBBO, SCBBO, Superior Iterations

1. INTRODUCTION

Optimization problems deal with the situations in which it is mandatory to search for the most appropriate solution among all the available solutions of a particular problem in a reasonable amount of time. These large scale optimization problems often suffer from the problems of multi-modality, non-continuous, dimensionality, non-convex and so-on. So, to tackle these real world complicated problems, efficient optimization algorithms are urgently required. Therefore, various evolutionary techniques have been developed and applied in recent years which include Genetic Algorithms (GAs), Particle Swarm Optimization algorithm (PSO), Differential Evolution algorithm (DE), Ant Colony Optimization (ACO), Artificial Bee Colony Strategy (ABC), and BBO (Simon, 2008).

From the last decade or so, the recent advances in theories and applications of nonlinear dynamics especially chaotic maps have drawn much attention in many fields of optimization in replacing certain algorithm dependent parameters (Jalili, Hosseinzadeh & Kaveh, 2014; Li-Jiang & Tian-Lun, 2002; Talatahari, Azar, Sheikholeslami & Gandomi, 2012). Chaotic maps have shown increase in population diversity and high level of mixing capability. Therefore, replacing a fixed parameter with

DOI: 10.4018/IJAMC.292520 *Corresponding Author

the chaotic map may provide solutions with higher mobility and greater diversity. Many chaotic maps have been used by these meta-heuristic algorithms to improve upon the results of these algorithms through proper balance between exploration and exploitation activities (Li-Jiang & Tian-Lun, 2002; Talatahari, Azar, Sheikholeslami & Gandomi, 2012; Yang, Li & Cheng, 2007).

Mingjun & Huanwen (2004) presented a novel algorithm by replacing the Gaussian distribution of simulated annealing with chaotic initialization and chaotic sequences. The proposed algorithm has been validated on typical complex function optimization problems. Alatas, Akin & Ozer, (2009) have presented twelve chaos-embedded PSO methods with the use of eight chaotic maps and analysed them on the benchmark functions. The simulation results demonstrated the robustness of the proposed methods with increased solution quality, i.e., in some cases they improved the global searching capability by escaping the local solutions. Alatas (2010a) presented two new ABC algorithms in combination with seven chaotic maps for parameter adaptation for improved convergence characteristics and to prevent the ABC from plunging into local solutions.

Alatas (2010b) presented seven new harmony search algorithms which employ chaotic maps for better convergence characteristics. In this research work, chaotic number generators are employed whenever there is a need for it by the classical harmony search algorithm. It has been demonstrated that results obtained from these coupling of various areas, like those of harmony search and complex dynamics, can significantly improve the quality of results in some optimization problems. Gharooni-fard et al. (2010) introduced a novel chaos based genetic based algorithm. The proposed approach, when applied to both balanced and unbalanced workflow structures, have validated its usage. Basically, the proposed approach scatters the solutions among the whole search space by employing the positive characteristics of the chaotic variables which together with avoiding premature convergence of the solutions also generates superior results within a shorter time.

Talatahari et al. (2012) proposed improved imperialist competitive algorithm using chaotic maps. Particularly, the random coefficient vector has been replaced by different chaotic systems and the random parameter in the orthogonal vector. Logistic and Sinusoidal maps performed better than the other chaotic maps used in this study. Gandomi et al. (2013) presented an upgraded variant of firefly algorithm by embedding 12 chaotic maps to tune the attractiveness and absorption coefficients. The proposed algorithm applied on the global optimization problems clearly demonstrated that some chaotic maps have phenomenally outperformed the results of the original firefly algorithm. Arul et al. (2013) proposed to solve the economic load dispatch problem with the application of chaotic firefly algorithm. In this paper, chaotic tent map was used to enhance two key parameters of firefly algorithm, i.e., randomization and attractiveness. The proposed algorithm demonstrated good convergence attributes on all considered economic load dispatch test cases in comparison to all the other soft computing techniques employed in the paper.

Fister et al. (2014) presented a randomized firefly algorithm in collaboration with different probability distributions and chaotic maps. The experimental results showed improved performance of the randomized firefly algorithm when used with probability distributions (e.g., uniform, Gaussian and l`evy flights) and chaotic maps (logistic and tent). Wang et al. (2014) presented a hybridized version of chaos theory with Krill Herd algorithm for solving optimization problems. Different chaotic maps were utilized to regulate the key parameter of Krill Herd algorithm. The experimental results on different chaotic Krill Herd variants established the superior performance of the singer map in forming the best chaotic Krill Herd. Taking clue from success of these metaheuristic algorithms, another popular algorithm in the series of nature inspired algorithms, BBO was introduced.

BBO was an evolutionary optimization algorithm which was given by American scientist, Dan Simon in 2008 (Simon, 2008). He invented a new population-based search technique which was inspired from the theory of island biogeography known as Biogeography-Based Optimization algorithm. The main characteristics of BBO algorithm are migration, speciation and extinction of species in a given geographical location. It is comparable to other evolutionary algorithms in solving complex optimization problems and afterwards, a lot of improvements have been given in the literature especially when chaos was incorporated in it (Lesmoir-Gordon & Rood, 2014; Saremi & Mirjalili, 2013).

So, chaotic migration and chaotic mutation operators are used to increase the population diversity to avoid entrapment of the candidate solutions in local optima (Liu et al., 2005). Saremi and Mirjalili (2013) used three chaotic maps with four benchmark functions to improve the weaknesses of the BBO algorithm. The integration of chaotic maps with the BBO algorithm is another method in improving the results of the BBO algorithm. Sine map have successfully improved the results out of all the other chaotic maps. Afterwards, they used ten chaotic maps with ten test functions in further expansion of their work (Saremi, Mirjalili & Lewis, 2014). They used this technique of integration in five different ways. Selection, migration and mutation operators are defined with chaotic maps at first, then combination of selection and migration and at the end they employed combination of selection migration and mutation strategies. Zhu, Luo and Zhu (2014) proposed improved genetic algorithm with four local search operators which are inspired from Dijkstra's algorithm and carried out when the topology changes to generate local shortest path trees which in turn are used to promote the performance of the individual in the population for dynamic shortest path problems. The experimental results obtained when applied on CEC 2014 test suite adapt rapidly to new environments and produce high quality solutions after environmental adjustments. Later on, Guo-ping et al. (2016) used chaotic maps with BBO algorithm in finding parameters of discrete chaotic systems with minimal time series data and control chaos using constant feedback method. Giri et al. (2017) used chaotic maps in improving local and global parameters and have shown increased convergence over the non-chaotic approach.

Jalili et al. (2014) used chaotic migration and chaotic mutation operators to solve the problem of truss structures with natural frequency constraints which are nonlinear dynamical optimization problem with several local optima. Later, Heidari, Mirvahabi & Homayouni (2015) used this technique in predicting earthquake-originated slope displacements (EIDS). They used chaotic BBO in combination with SVR (Support Vector Regression) to investigate the best possible values of SVR parameters. Wang et al. (2016) used this combination of chaos with BBO in centroid based clustering methods. They used three types of simulation data in proving the superiority of their approach. Wang and Song (2017) used chaotic mapping strategy in combination with BBO optimal migration model which is close to the natural law in achieving overall increased convergence velocity and higher optimization precision accuracy. To know more about the BBO algorithm, its modifications and its combination with other meta-heuristic algorithms, one may go for a comprehensive survey from the last ten years prepared by Ma et al. (2017). Some of the other researchers who have contributed to the chaos based metaheuristic algorithms have been given in Table 1.

A number of different chaotic maps have been used in the BBO algorithm in the previous researches (Saremi & Mirjalili, 2013; Saremi, Mirjalili & Lewis, 2014). In this paper, we propose to use the chaotic sequence that is generated by alternating two ordered logistic maps together in the superior orbit and then evaluate their performance to ascertain how they behave in increased solution space. The paper has been structured as follows. Section 2 explains the motivation and thought behind this paper. Section 3 discusses the preliminaries of the BBO algorithm, Parrondo's paradox and its applications in superior orbit. Section 4 describes about the proposed approach of combining alternating strategy in superior orbit with chaotic BBO and also the theoretical time complexity of the proposed approaches. Section 5 gives the simulation experiments and results analysis followed by concluding remarks which are discussed in Section 6.

2. MOTIVATION

The quality of random sequences generated remarkably affects the global optimal solutions of metaheuristic algorithms. Previous studies have shown that these random sequences with an advanced amount and uniform structure are vital to achieving the globally optimal results with enhanced

Table 1. A brief summary of chaos based metaheuristic techniques

Name	Method/Algorithm	Chaotic maps and Benchmarks/ Datasets Used	Parameters Validated	Applications
Yakubu, & Aboiyar (2018)	New confusion-diffusion cryptosystem which makes use of chaos rich Schimizu-Morioku system to shuffle the image	Shimizu-Morioka system and a standard test digital colour image of size 256x256, stored with TIF file format (Lena_colour.tif)	Histogram uniformity analysis, the correlation coefficient analysis, and the number of pixel changing intensity	Image segmentation problems
Linglong, Yehui, & Changkai (2018)	Conventional fuzzy clustering algorithms with global search capability of the *PSO* swarm algorithm along with chaotic sequences	Logistic map and three test images in tiff format are used for image segmentation	Time consumption and classification accuracy	Image classification problems
Wang et al. (2018)	Chaotic starling *PSO* which is inspired from the collective responses of the starling birds	Logistic map and benchmark functions are Sphere, Griewank, Rastrigin, and Rosenbrock and datasets are Data_3_2, Data_5_2, Data_10_2, Data_4_2, Iris, Wine, Glass, and CMC.	Robustness and effectiveness	Optimization problems
Bejinariu et al. (2019)	*PSO*, multi swarm optimization (*MSO*), cuckoo search algorithm (*CSA*) and black hole algorithm (*BHA*) are combined with nine chaotic maps	Chebyshev, Circle, Gauss, Iterative, Piecewise, Sine, Singer, Sinusoidal and Tent maps and Medical dataset	Precision of clusters	Clustering problems
Gálvez, Cuevas, Becerra & Avalos (2019)	Cluster chaotic optimization	*ICMIC* map and 30 benchmark functions and 4 engineering design optimization problems	Robustness and accuracy	Optimization problems
Lu et al. (2019)	Dynamic swarm firefly algorithm in combination with chaos theory and max-min distance algorithm	Tent map and Iris, Wine, Seed, Glass, Hayes-Roth, and New-Thyroid.	Fast convergence, accuracy of clustering results and avoidance of local solutions	Optimization problems
Arslan & Toz (2019)	Whale optimization algorithm along with chaotic maps using an adaptive normalization method and fuzzy *c*-means clustering algorithm	Chebyshev, Circle, Gauss, Iterative, Logistic, Piecewise, Sine, Singer, Sinusoidal, and Tent maps and 13 benchmark functions and Iris, Balance Scale, User Modeling, Breast Cancer, Seeds, and Fertility dataset	Clustering performance	Optimization problems
Bouyer & Farajzadeh (2015)	A hybrid of *k*-harmonic means clustering algorithm and a modified version of *PSO* algorithm along with Cuckoo Search Levy Flight algorithm	ArtSet1, ArtSet2, Iris, Wine, Wisconsin breast cancer, Ripley's glass, CMC, Thyroid gland, Vowel, Ecoli	Convergence rate, efficiency and local optima entrapment	Clustering optimization problems
Dhanusha, & Kumar (2021)	Unsupervised nature inspired crow search learning model	Logistic map and "*CASAS*" and "*OASIS*" datasets	Efficiency of the proposed algorithm in handling the noisy data and indeterminacy behaviour of the dataset	Alzheimer disease detection
Zhu, Liu, & Wang (2020)	Chaotic crow search algorithm and improved fuzzy *c*-means clustering algorithm	Chebyshev map and Synthetic and non-destructing images	Cluster density and noise reduction	Image segmentation
Kaur, Pal & Singh (2020)	Flower pollination algorithm with chaos	Logistic map, Sine map, Dyadic map, Chebyshev map, and Circle map and Iris, Wine, Breast_Cancer, Glass, Balance, Dermatolgy, Haberman, Ecoli, Heart, Tae, Spambase, ILPD, Leaf, Libras, Qualitative_Bankruptcy, Synthetic are the datasets employed.	Execution time, stability and convergence speed	Optimization clustering problems
Singh (2020)	Harris hawk optimization algorithm in relation with chaotic sequences	Logistic map and Shape datasets are Aggregation, Compound Path based, Spiral, Flame, Jain, *R*15, *D*31 and UCI datasets are Glass, Iris, Wine, Yeast	Accuracy of cluster indices	Clustering applications

continued on next page

Table 1. Continued

Name	Method/Algorithm	Chaotic maps and Benchmarks/ Datasets Used	Parameters Validated	Applications
Jin, Lin & Zhang (2021)	Traditional *k*-means clustering algorithm with chaos based artificial bee colony approach	as chaotic map and benchmark functions are Alpine, Schwefel 2.22, Schwefel 2.21, QuarticWN, Quartic, Sum Power, Shifted Sphere, Step, Zakharov, SumQuares, SumDifference, Schwefel 2.26, Shifted Rosenbrock, Schwefel 1.2, Ackley, Griewank, Rastrigin, Schaffer, Rosenbrock, Sphere and datasets are Iris, Balance Scale, Glass, Wine, Ecoli, Abalone, Musk, Pendigits, SkinSeg., *CMC*, Cancer	Improved accuracy of solutions and processing efficiency	Clustering optimization problems
Fang et al. (2021)	Chaotic cross iterative kernel *k*-means enhanced with image classification and similarity measurements	Cross iterative kernel and *PVAG*, *PVPS*, and *CDD* datasets are used	Cluster classification	Plant disease image identification
Han et al. (2021)	Control and anti-control of chaos based on largest Lyapunov exponent which is moving with the method of reinforcement learning	Lorènz map and Hènon map and datasets are obtained from these two maps for control and anti-control of chaos	Lyapunov exponent	Identification of chaotic dynamical systems

accuracy. From a few years, it has been seen that the use of chaotic sequences instead of random numbers have been quite instrumental in substantially increasing the performance of the various metaheuristic algorithms. This suggests that the use of chaos in metaheuristic algorithms is an area of great interest among many researchers from disciplines of varying fields (Pecora & Carroll, 1990; dos Santos Coelho & Mariani, 2008; Strogatz, 2018; Jin, Lin & Zhang, 2021).

In the context of ecological modelling, from the last decade or so, the idea of switching strategies has been reconsidered in the form of Parrondo's paradox, where two losing games when combined together in a deterministic or random order give a winning game (Danca, Fečkan & Romera, 2014). Logistic map, over the years have served as a medium for development and understanding of nonlinear dynamics. Therefore, the idea of using alternate discrete dynamics on logistic map may yield favourable situations. One of the situations may be when two ordered logistic maps are alternated together, it may result in chaotic behaviour which is an ideal condition for achieving higher rates of optimization values in optimization problems, i. e., "$order_1 + order_2 = chaos$". For more details, one may refer to (Danca, Fečkan & Romera, 2014; Danca & Tang, 2016; Levinsohn, Mendoza & Peacock-López, 2012; Maier & Peacock-López, 2010; Peacock-López, 2011). Later on, Rani and Yadav (Rani & Yadav, 2016; Yadav & Rani, 2015) extended this idea in studying logistic map and its variants in superior orbit and given examples of "$chaos_1 + chaos_2 = order$" and "$order_1 + order_2 = chaos$" (vice-versa).

3. PRELIMINARIES

3.1. Biogeography Based Optimization

The term BBO suggests that it has its roots in the biogeography discipline which concerns with the relationships between different species (habitants) living in ecologically distributed habitats in a given ecosystem. The evolvement of the species happens in terms of immigration, emigration and mutation activities. The drifting of the species to neighbouring habitats takes place through various means like air, water, and many other different pathways (Wallace, 2005).

Additionally, in relation to movement of species between different habitats, each habitat is having its own set of survival indicators, which is called as Habitat Suitability Index (HSI). In fact, BBO being an optimization algorithm in which a habitat is taken as a possible candidate solution. The variables that characterize habitats are called Suitability Index Variables (SIVs). The fitness value of each habitat is calculated using HSI (MacArthur & Wilson, 2016).

High HSI habitats tend to have higher number of species, while lower HSI habitats attract smaller number of species. The HSI of poor habitats can be improved with new features derived from more attractive habitats in the evolution process (Simon, 2011). In this approach, the information between poor and good habitats is shared through the migration operator. This migration operator is responsible for emigration and immigration. This adaptive information sharing between habitats happens due to immigration rate λ and emigration rate μ of each habitat which in turn are functions of the number of species present in the habitat. These can be calculated according to the following equations as (Du, Simon & Ergezer, 2009; Giri et al., 2017):

$$\lambda_k = I\left(1 - \frac{K}{S_{max}}\right) \tag{1}$$

$$\mu_k = E\left(\frac{K}{S_{max}}\right) \tag{2}$$

where I . is representing the maximum possible immigration rate; E is showing the maximum possible emigration rate; the number of species in the k^{th} habitat is represented by K and the maximum number of species supported by the habitat is represented by S_{max} (Guo-ping et al., 2016; Heidari, Mirvahabi & Homayouni, 2015). The pseudo code of the BBO algorithm is following.

Algorithm 1. Pseudo code of BBO algorithm (Saremi, Mirjalili & Lewis, 2014)
Step 1. Initialize the parameters of BBO algorithm.
Step 2. While the termination condition is not satisfied.
Step 3. Initialize the Fitness Function for the Habitats.
Step 4. Calculate the Habitat Fitness Index (HSI) and sort them.
Step 5. Update the S, λ and μ of each habitat.
Step 6. For i=1 to maximum number of habitants do
If rand < λ_i then
For j=1 to maximum number of habitants do
If rand < μ_j
Select a random habitant in x_i and replace it with x_j
End if
End for
End if
End for
If rand < mutation probability
Mutate a random number of habitats
End if
Elitism
End while

Fig. 1 illustrates the linear migration model of the BBO algorithm. As it is clear from the figure that the emigration rate is zero when there are no species present in the habitat. The emigration rate attains the maximum value E when the species reach to its maximum capacity S_{max}. In the similar manner, the immigration rate achieves the maximum possible value I when the number of species is zero. Also, when the number of species becomes S_{max}, then the immigration rate declines and becomes zero. S_0 is the equilibrium point, which is achieved when the emigration rate μ becomes equal to immigration rate λ (Simon, 2008; Simon, 2011).

Figure 1. Immigration (λ) and Emigration curves (μ)

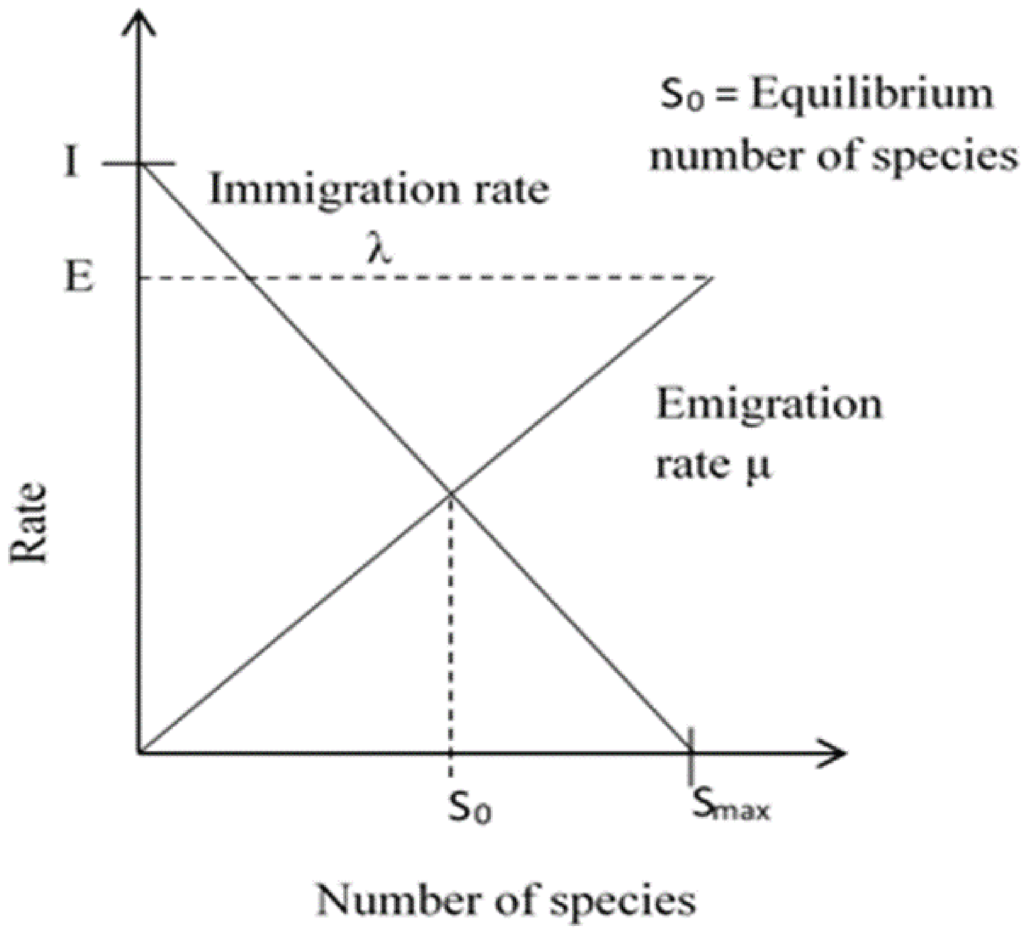

For each individual habitat H_k, the associated probabilistic rate which determines whether to immigrate or not is λ_k. Based on the emigration rate μ_j, the emigrating solution H_j is selected probabilistically when immigration is selected. During replacement of a copy of SIV σ from individual habitat H_j to H_k, it is said that σ has immigrated to H_k and emigrated from H_j; that is $H_k(\sigma) \leftarrow H_j(\sigma)$. Thus migration operator is able to efficiently enhance the global convergence of the algorithm by sharing information among individual habitats (Wallace, 2005).

After migration activity, mutation operator is used to further increase the diversity of the available population. It is a probabilistic operator which is used to modify the SIV of a randomly selected habitat which is habitat's priori probability of existence and is computed as follows (Heidari, Mirvahabi & Homayouni, 2015; Jalili, Hosseinzadeh & Kaveh, 2014).

$$m_k = m_{max}\left(1-\frac{P_k}{P_{max}}\right) \tag{3}$$

where m_{max} represents a user-defined parameter and $P_{max} = \max\left\{P_k\right\}, k = 1,2,3,\ldots,N$ and P_k shows the probability that the habitat has exactly k number of species.

Another feature of BBO is that the habitats having higher HSI are kept as elites and moved from the previous generation to the next generation. It is meant therefore that the new habitats of current iteration are combined with some elites of the prior generation. After combination, the higher HSI are selected for creation of newer generation of population. In this study, the probability of mutation rate is set to 0.005 (MacArthur & Wilson, 2016; Simon, 2008; Simon, 2011).

3.2. Parrondo's Paradox

It is a paradox in game theory given by famous physicist Juan Parrondo in the year 1996. As per this paradox, when two simple games with negative gains are played together alternatively may produce a game with positive gains in a different deterministic or random manner (Danca, Fečkan & Romera, 2014). In 2001, it was introduced to the combination of two unstable systems A_1 and A_2 to study the dramatic change in the properties of the systems when they are combined. Initially, the authors considered the traditional idea of Parrondo's paradox of "*losing*$_1$ + *losing*$_2$ = *winning*" and applied it on different kinds of linear systems to show the "*instability*$_1$ + *instability*$_2$ = *stability*" (Danca & Tang, 2016; Mendoza et al., 2018).

Two different discrete dynamics A_1 and A_2 are considered and the alternation of combination of the dynamical systems A_1 and A_2 is discussed as follows:

$$x_0\ A_{H0}x_1\ A_{H1}x_2\ A_{H2}x_3\ \ldots,$$

where H is describing a deterministic or random law which allocates a value of 1 or 2 to every member of the sequence {0, 1, 2……}, and $\{x_0, x_1, x_2 \ldots\}$ are values given to a variable x which is representing the physical system. The two individual dynamics A_1 and A_2 may be chaotic but when combined periodically in an alternated way $A_1A_2A_1A_2A_1A_2 \ldots\ldots = \left(A_1A_2\right)$, may produce an ordered sequence and vice versa. The phenomenon thus created can be stated in terms of "*chaos*$_1$ + *chaos*$_2$ = *order*" and "*order*$_1$ + *order*$_2$ = *chaos*" (vice-versa) (Levinsohn, Mendoza & Peacock-López, 2012).

Definition: Alternated System: Let us consider two different dynamics A_1 and A_2, where A_1: $x_{n+1} = x_n^2 + c_1$, A_2: $x_{n+1} = x_n^2 + c_2$, and the alternation of combination of two dynamics A_1 and A_2 is defined as:

$$x_{n+1} = \begin{cases} x_n^2 + c_1, & when\, n\, is\, odd, \\ x_n^2 + c_{2,} & when\, n\, is\, even. \end{cases} \tag{4}$$

where x, c, c_1, c_2 represent the real numbers. As it is a well-known fact that $x_{n+1} = x_n^2 + c$ is topologically conjugate to the logistic map $x_{n+1} = rx_n\left(1-x_n\right)$, $x_n \in \left[0,1\right]$, it is derived that there may be a situation that shows "*chaos*$_1$ + *chaos*$_2$ = *order*" and also "*order*$_1$ + *order*$_2$ = *chaos*" which may arise in the logistic map. For more details on the literature on Parrondo's paradox, one may refer to (Danca, Fečkan & Romera, 2014; Danca & Tang, 2016; Levinsohn, Mendoza & Peacock-López, 2012).

3.3. Superior Orbit (*SO*)

Feedback processes discovered by Isaac Newton and Gottfried W. Leibniz have found tremendous applications in nonlinear systems in the form of dynamical laws (Ashish, 2014). The feedback process is the process in which the output of the first iteration is given to the second iteration and the process is repeated until some given number of iterations. It is simple in principle as the same process is repeated again and again. Mostly, two types of feedback machines are used.

3.3.1. One-step Feedback Machine (Picard Orbit)

Definition: (Picard Orbit): Let A be a non-empty set of numbers and $f : A \to A$. For a point, x_0 in A, the Picard orbit (generally called orbit of f) is the set of all iterates of the point x_0, that is,

$$O\left(f, x_0\right) = \left\{x_n : x_n = f\left(x_{n-1}\right), n = 1,2,\ldots\right\}. \tag{5}$$

The orbit $\left(O\left(f, x_0\right)\right)$ of f at the initial point x_0 is the sequence $\left\{f\left(x_0\right)\right\}$ (Ashish, 2014; Goel, 2011; Negi & Rani, 2008a and 2008b).

3.3.2. Two-step Feedback Machine (Superior Orbit)

Two-step feedback machine was introduced by Rani in fractal and chaotic models until recently (Negi & Rani, 2008). It became the reason for generation of superior fractals. In this approach, a new number is generated after the insertion of two numbers, and the formula for computing the new number is $x_{n+1} = g\left(x_n, x_{n-1}\right)$.

Definition: (Superior Iterates): Let A be a subset of real numbers and $f : A \to A$. For $x_0 \in A$, construct a sequence $\left\{x_n\right\}$ in the following manner:

$$x_1 = \beta_1 f\left(x_0\right) + \left(1 - \beta_1\right) x_0 ,$$
$$x_2 = \beta_2 f\left(x_1\right) + \left(1 - \beta_2\right) x_1$$

$$x_n = \beta_n f\left(x_{n-1}\right) + \left(1 - \beta_n\right) x_{n-1} \tag{6}$$

where $0 < \beta_n \le 1$ and $\left\{\beta_n\right\}$ is convergent away from 0 (*c.f.* Negi & Rani, 2008a).

The subset A may also be taken as a subset of complex numbers without loss of generality as depicted in the above definition. The sequence constructed above $\left\{x_n\right\}$ is a superior sequence of iterates or superior orbit, denoted as $SO\left(f, x_0, \beta_n\right)$. . Superior orbit at $\beta = 1$ reduces to $O\left(f, x_0\right)$ (see above definition of Picard orbit). The definition is originally given by W. R. Mann (1953). M. A. Krasnosel'skii (1955) gave superior iterates for $\beta_n = 0.5$. Because of the superset of solutions that are generated as compared to Picard iterates by Mann iterations, Rani and Kumar renamed them as superior iterates (Ashish, 2014; Goel, 2011; Singh, Mishra & Sinkala, 2012).

A number of superior fractal structures have been developed by Rani along with other researchers for $\beta_n = \beta, n = 1,2,\ldots\ldots$ for various values of β (Negi & Rani, 2008a; Negi & Rani, 2008b; Negi, Rani & Mahanti, 2008).

4. ALTERNATED SUPERIOR CHAOTIC BBO (ASCBBO) AND SUPERIOR CHAOTIC BBO (SCBBO)

The alternate superior chaotic mapping strategy is employed to realize the mutation operator in BBO algorithm and we call the proposed algorithm as alternated superior chaotic BBO, abbreviated as ASCBBO algorithm. The integration of alternated chaotic BBO in superior orbit with mutation can help in improving the detection capability (exploitation) by the increased solution set with these kinds of combinations. The ASCBBO is used with different standard test functions which are Sphere, Schwefel, Rosenbrock, Quartic, Penalty #1, Penalty #2, Griewank, Fletcher, Ackley and Rastrigin (Saremi, Mirjalili & Lewis, 2014). A habitat for migration is selected on probability which is defined by selection operator (λ) and after the selection of a habitat; emigration is performed with emigration probability (μ) as can be seen from Fig. 1. The chaotic sequence $C(x)$ is generated when we iterate the logistic map $f\left(x\right) = r * x * \left(1 - x\right)$ in an iterative manner by taking the values of r as 4.76 and 4.8034 in a superior orbit with $\beta = 0.7$ in odd and even iterations respectively. These values have been obtained from the work of Yadav (Yadav & Rani, 2015). The logistic map shows ordered (non-chaotic) behaviour when these values are iterated individually. However, when these values of 'r' are iterated alternatively, then the map produces chaotic oscillations, i.e., $order_1 + order_2 = chaos$. In case of superior chaotic BBO (SCBBO), the value of r is taken as 4.1 and $\beta = 0.9$ in a superior orbit as given by Rani and Agarwal (2009). The mapping of chaotic sequences to mutation operators is described further as follows.

4.1. Chaotic Mapping of Mutation Operator

When the selection and emigration of the habitat is done, then the next task is to mutate the inhabitants so that the stagnation of the species is removed by altering certain parameters of the species to further diversify the population in order to get more areas of favourable solution space for enhancement of the required procedure. The chaotic values are used to describe this mutation probability as described below.

for i = 1 to number of habitants at k-th habitat
if $C(x) <$ *Mutation_rate* (k) *then*
Mutate i-th habitant
end if
end for

Here, $C(x)$ is representing the chaotic values of the map at t^{th} iteration and *Mutation_rate* (k) is illustrating the mutation probability of k^{th} habitat. The chaotic mapping gives the values for the emigration operators which are in the range [-1, 1] and then are normalised in the range of [0, 1] (Saremi, Mirjalili & Lewis, 2014). The investigation of BBO and ASCBBO under the influence of chaotic maps is explained in the following section. The initial value of ASCBBO is kept at 0.7 as in case of CBBO (Saremi, Mirjalili & Lewis, 2014) as it holds great significance in case of nonlinear chaotic situations.

The comparative study of all the graphs given in Fig. 2 clearly indicates that in case of superior logistic map, the chaotic data points are densely populated and more uniformly distributed which may help in finding more global optimal values as the solution space is increased for the candidate particles. In case of alternated superior chaotic logistic map, two chaotic maps are used in an alternate manner in the increased solution domain of finding a possible global optimal point which further increases the possibility of avoidance of the candidate solutions in local optimal points as the increased complexity in the alternated chaotic maps further reduces the biasness in input data.

4.2. Theoretical Time Complexity of BBO, CBBO, ASCBBO, and SCBBO

As compared with other metaheuristic algorithms, BBO works by sharing information among candidate solutions which makes it suitable for similar kind of solving problems that the other algorithms are

Figure 2. Chaotic data plots of different chaotic maps

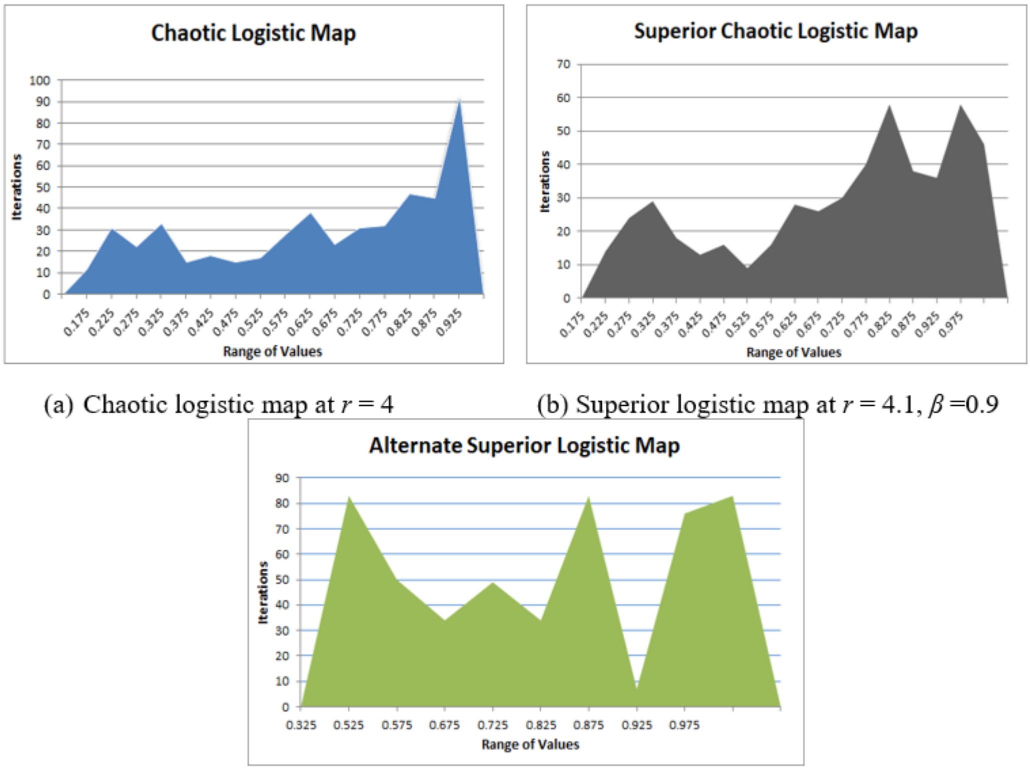

(a) Chaotic logistic map at $r = 4$

(b) Superior logistic map at $r = 4.1$, $\beta = 0.9$

(c) Alternate superior logistic map at $r_1 = 4.76$, $r_2 = 4.8034$, $\beta = 0.7$

used for, such as when applied on high dimensional data. Hence, the computational cost of BBO and other similar algorithms will be the same as they heavily rely on the evaluation of the objective function. BBO uses tournament selection for the selection operator which usually demands $O(N)$ time complexity, where N is the number of the habitats. For migration operation, a habitat having D number of SIVs demands $O(ND + O(f))$ time complexity where $O(f)$ is the time complexity for computing the fitness function f. Therefore, each generation needs $O(N(ND + O(f)))$ time for its computation. Constant time is required when the neighbourhood HSI is selected. Hence, when M number of iterations are used in an experiment, then the required time becomes $O(NM(ND + O(f)))$. Following observations are made for the general time complexity of BBO algorithm.

1. $O(f)$ is considered much less as compared to N^2, then the overall time complexity of the BBO algorithm becomes $O(M N^2 D)$.
2. When D is insignificant compared to N, then the complexity of BBO takes the form as $O(M N^2)$.

In essence, whenever a habitant in a habitat immigrates, then the emigration vector is computed which depends upon the local best (local population) and global best (whole population), based on the rate of migration (Giri et al., 2017). Also in case of CBBO, SCBBO and ASCBBO, different chaotic sources are used for the selection, migration and mutation of the habitants which also require constant time as the case with the random. Hence, the time complexity of CBBO, SCBBO, and

ASCBBO is equivalent to BBO. Thus, for small number of SIVs, the overall time complexity of all the versions of BBO is $O(M\,N^2)$.

5. SIMULATION EXPERIMENTS AND RESULTS ANALYSIS

Ten standard benchmark functions and CEC 2014 test suite (in 50 dimensional space) have been used to test the performance of the ASCBBO and SCBBO algorithms. These test functions have been categorized into two groups namely unimodal and multimodal test functions. As the name specifies, unimodal functions have single optima in them which makes them best suited for the exploitation related activities. On the other side, multimodal functions have multiple optimal points which create challenges in finding the most appropriate optima in these kinds of test functions. Because one of them is a global optima and rest all are the local ones. The avoidance of local optimal points is the characteristic property of any metaheuristic algorithm in finding global values. Hence, the multimodal functions are given the task of exploring more region(s) in order to find the global optimal points. Thus, this piece of research work is applicable to both single objective and multi-objective test problems. It is to be noted that all the test functions used in this study have the minimal value 0 except for Schwefel function which is having a minimal value as -12569.5. Table 2 shown below is describing the various properties of the different unimodal and multimodal functions. The dimension of these functions is shown as Dim which gives the count of various parameters used in the function. Range is depicting the boundary of the search space of the test function (Saremi, Mirjalili & Lewis, 2014). Various initial parameters used for the BBO, CBBO, SCBBO, ASCBBO, Grey Wolf Optimizer (GWO), Sine Cosine Algorithm (SCA), Ant Lion Optimizer (ALO), Genetic Algorithm (GA), Differential Evolution (DE), Ant Colony Optimization (ACO), Gravitational Search Algorithm (GSA) approaches are listed in Table 3.

5.1. Performance Analysis of ASCBBO and SCBBO

All the simulation experiments have been done in Matlab R2016a. The proposed algorithms are run ten times and the average is computed. Each time 500 iterations are being performed for the mutation operator on simple BBO and ASCBBO. In case of CEC 2014 benchmark functions, 1000 iterations have been carried out on each and every algorithm. The best values for average (mean) and standard deviation obtained in the last iteration for both the operators are observed and depicted in Tables 4 and 5. Notice that the ASCBBO shows much improvement in mean optimal values in both the cases as listed in Tables 4 and 5 when compared to CBBO (Saremi, Mirjalili & Lewis, 2014). Also the standard deviation values are showing the same trend.

In case of plain BBO operator as shown in Table 4, Penalty #2 test function gave the best values as compared to other benchmark functions. The other test functions Penalty #1, Fletcher, Rosenbrock, Schwefel, Sphere, Rastrigin, Griewank, Ackley and Quartic follow the descending sequence in terms of mean values. Same trend is also repeated by standard deviation values except for Griewank and Penalty #2 test functions. The decreasing order of standard deviation values is Penalty #1, Fletcher, Rosenbrock, Schwefel, Rastrigin, Sphere, Quartic, and finally Ackley test function.

The mutation operator shown in Table 5 follows the descending sequence of mean values as Penalty #1, Penalty #2, Fletcher, Rosenbrock, Schwefel, Griewank, Sphere, Quartic and Ackley test functions except in case of Rastrigin. In the same manner, Penalty #2 predicted the best standard deviation value in case of mutation probability followed by Penalty #1, Fletcher, Schwefel, Rosenbrock, Griewank, Sphere, Quartic and in the end Ackley test function except Rastrigin test function.

In case of CEC 2014 test functions also, when comparison has been made with state of the art algorithms like Grey Wolf Optimizer (GWO), Sine Cosine Algorithm (SCA), Ant Lion Optimizer (ALO), Genetic Algorithm (GA), Differential Evolution (DE), Ant Colony Optimization (ACO), Gravitational Search Algorithm (GSA), our methods (ASCBBO and SCBBO) have performed phenomenally well and outperformed all the compared algorithms with much less mean and standard deviation values as given in Tables 6 and 7.

Thus from above discussion, it is quite clear that ASCBBO and SCBBO have given much improved results as compared to CBBO (Saremi, Mirjalili & Lewis, 2014). These methods can also be employed on parameter optimization for the prediction of a number of practical problems like software testing, software fault prediction, Glaucoma, Covid-19, glucose, mammography, cardiac problems, and plant leaf disease etc. (Khanna, Chauhan & Sharma, 2019; Khanna et al., 2019; Singh, Khanna & Garg, 2020; Thawkar, Singh & Khanna, 2021; Singh, Garg & Khanna, 2021)

5.2. Qualitative Analysis

Line graphs have also been plotted in the two cases of BBO and its mutation probability for computing the qualitative analysis of ASCBBO algorithm as given in Figs. 3 and 4. In each of the graphs shown in both the figures, the mean values are plotted against the number of iterations with respect to the particular benchmark function. All the graphs show higher rates of convergence in both the cases as compared to CBBO with respect to given test functions once again proving the superior performance of ASCBBO algorithm. Also, the convergence plots and box plots (Anova test) given in Figs. 5 and 6 clearly indicate the superior performance of our techniques on CEC 2014 test functions as they have been able to avoid local optimal solutions with high speed and accuracy of solutions.

5.3. Statistical Testing

Statistical tests should be conducted on the meta-heuristic algorithms to test their performance as proposed by Derrac et al. (2011). Mere computing the mean and standard deviation values are not enough in terms of overall inductiveness of the validity of the performance of these algorithms. Therefore, a nonparametric statistical test, which is Wilcoxon's rank sum test, (Wilcoxon, 1992) should be carried out to test the validity of the metaheuristic algorithms separately. The significance level of the test is kept at 5%. It is a general practice that the p values less than 0.05 are considered to be sufficient enough against the theory of null hypothesis. Also, the p values depicted in Tables 3 and 4 in both the cases have proved the validity of the ASCBBO and SCBBO algorithms.

6. CONCLUDING REMARKS

In this paper, the use of chaotic sequence in an alternated manner in superior orbit is used as a source of population initialization. These have been used in selection, emigration, mutation and their combination stages. Chaotic maps in superior orbit produce more uniformly distributed chaotic sequences than used in chaotic BBO. Use of two chaotic attractors alternatively increase the complexity in chaotic sequences. Both the ways reduce biasness in the input chaotic data which helps the candidate solutions to arrive at global optimal points without being fallen in local optima and stuck there with much improved speed and precision of resultant solutions.

In all the cases, ASCBBO and SCBBO have been able to achieve much higher levels of optimization in comparison to CBBO. All the state of the art algorithms used in case of CEC 2014 test functions namely GWO, SCA, ALO, GA, DE, ACO and GSA are compared on the parameters: mean, standard deviation and p value test. In some cases, the dip in values of optimal points in case of ASCBBO and SCBBO approaches are multi time than the compared algorithms. Thus, both theoretically and statistically, we have proved categorically that the methods suggested in this paper have been able to avoid premature convergence and achieved higher solution accuracy along with enhanced performance against some of the well-known metaheuristic algorithms which are trending recently (GWO, SCA, ALO, GSA) and also the most popular previous algorithms (GA, DE, ACO).

Future Work: In future, it is going to be an interesting phenomenon to deploy this technique on real world engineering optimization problems and other combinatorial optimization problems which are inherently complex in nature. Also, this technique could be applied on other metaheuristic algorithms like Cuckoo Search, Grasshopper Optimization Algorithm, Whale optimization Algorithm, Salp Swarm Optimization Algorithm, Elephant Herding Optimization Algorithm and the like ones.

Table 2. Various benchmark functions used in the study

Sr. No.	Benchmark Functions	Function Formula	Dim	Range	Optimal Value (f_{min})	Features
F1	Sphere	$f\left(x\right)=\sum_{i=1}^{n}x_i^2$	30	[-100,100]	0	Unimodal, Separable, Regular
F2	Schwefel	$f\left(x\right)=\sum_{i=1}^{n}-x_i\sin(\sqrt{\lvert x_i\rvert})$	30	[-65.536,64.536]	-12569.5	Unimodal, Non-Separable, Regular
F3	Rosenbrock	$f\left(x\right)=\sum_{i=1}^{n-1}\left[\left(100(x_{i+1}-x_i^2\right)^2+\left(x_i-1\right)^2\right]$	30	[-2.048, 2.048]	0	Unimodal, Non-Separable, Regular
F4	Quartic	$f\left(x\right)=\sum_{i=1}^{n}\left[ix_i^4\right]$	30	[-1.28, 1.28]	0	Unimodal, Separable, Regular
F5	Penalty 1	$f\left(x\right)=\frac{\pi}{n}\left\{10\sin\left(\pi y_1\right)+\sum_{i=1}^{n}\left(y_i-1\right)^2\left[1+10sin^2\left(\pi y_{i+1}\right)\right]+\left(y_n-1\right)^2\right\}+\sum_{i=1}^{n}u\left(x_i,10,100,4\right)$ $y_i=1+\frac{x_{i+1}}{4}$ $u\left(x_i,a,k,m\right)=\begin{cases}k\left(x_i-a\right)^m & x_i>a\\0 & -a<x_i<a\\k\left(-x_i-a\right)^m & x_i<-a\end{cases}$	30	[-50, 50]	0	Multimodal, Non-Separable, Regular
F6	Penalty 2	$f\left(x\right)=0.1\left\{sin^2\left(3\pi x_1\right)+\sum_{i=1}^{n}\left(x_i-1\right)^2\left[+sin^2\left(3\pi x_i+1\right)\right]+\left(x_n-1\right)^2\left[1+sin^2\left(2\pi x_n\right)\right]\right\}+\sum_{i=1}^{n}u\left(x_i,5,100,4\right)$ $u\left(x_i,a,k,m\right)=\begin{cases}k\left(x_i-a\right)^m & x_i>a\\0 & -a<x_i<a\\k\left(-x_i-a\right)^m & x_i<-a\end{cases}$	30	[-500, 500]	0	Multimodal, Non-Separable, Regular
F7	Griewank	$f\left(x\right)=\frac{1}{4000}\sum_{i=1}^{n}x_i^2-\prod_{i=1}^{n}cos\left(\frac{x_t}{\sqrt{t}}\right)+1$	30	[-600, 600]	0	Multimodal, Non-Separable, Regular
F8	Fletcher	$f\left(x\right)=\sum_{i=1}^{n}\left(A_i-B_i\right)^2$ $A_i=\sum_{j=1}^{n}\left(a_{ij}sin\alpha_j+b_{ij}cos\alpha_j\right)^2,\ B_i=\sum_{j=1}^{n}\left(a_{ij}sinx_j+b_{ij}cosx_j\right)^2$	30	[-Π, Π]	0	Multimodal, Non-Separable, Irregular
F9	Ackley	$f\left(x\right)=-20\exp\left(-0.2\sqrt{\frac{1}{n}\sum_{i=1}^{n}x_i^2}\right)-exp\left(\frac{1}{n}\sum_{i=1}^{n}\cos\left(2\pi x_i\right)\right)+20+e$	30	[-50, 50]	0	Multimodal, Non-Separable, Regular
F10	Rastrigin	$f\left(x\right)=\sum_{i=1}^{n}\left[x_i^2-10\cos\left(2\pi x_i\right)+10\right]$	30	[-5.12, 5.12]	0	Multimodal, Separable, Regular

Table 3. Initialization of parameter values for BBO, CBBO, SCBBO, ASCBBO, GWO, SCA, GSA, ACO, GA, DE and ALO

Parameter initializations for BBO, CBBO, SCBBO and ASCBBO	**Value**
Size of population	30 (50 in CEC 2014 test problems)
Habitat modification probability	1
Immigration probability bounds per gene(inhabitant)	[0, 1]
Step size for numerical integration of probabilities	1
Maximum immigration (I) and Maximum Emigration (E)	1
Probability of Mutated inhabitants	0.005
Parameter initializations for GWO	**Value**
a (Area Vector)	2
r_1, r_2 (Random Vectors)	[0,1]
Size of population	50
Parameter initializations for SCA	**Value**
Size of population	50
a (Constant)	2
Parameter initializations for GSA	**Value**
Elitist Check (No. of fittest agents after stopping criterion)	1
Rpower (Exponent of distance between agents)	1
Min_flag (1: minimum ; 0: maximum)	1
Size of population	50
Parameter initializations for ACO	**Value**
Pheromone update constant	1
Initial pheromone	10
Pheromone sensitivity	0.3
Visibility sensitivity	0.1
Size of population	50
Parameter initializations for GA	**Value**
Size of population	50
Pc (Crossover probability)	0.95
Pm(Mutation probability)	0.001
Er (Elitism)	0.2
Parameter initializations for DE	**Value**
Size of population	50
Lower bound of scaling factor	0.2
Upper bound of scaling factor	0.8
PCR (Crossover probability)	0.8
Parameter initializations for ALO	**Value**
Size of population	50

Table 4. Performance comparison of ASCBBO on simple BBO operator

Name of the Function	Criteria	CBBO (Saremi, Mirjalili & Lewis, 2014)	ASCBBO
Sphere	Mean	50.19608	37.17486136
	Standard Deviation (SD)	17.88657	10.25978
	P-Value	0.427355	0
Ackley	Mean	16.93064	15.75670808
	Standard Deviation (SD)	1.259177	0.844094
	P-Value	0.212294	0
Griewank	Mean	142.9973	140.2411749
	Standard Deviation (SD)	28.83283	29.65174
	P-Value	0.57075	0.208754
Fletcher	Mean	828,365.4	603882.8685
	Standard Deviation (SD)	189,001	145286.3
	P-Value	0.001315	3.2819E-205
Schwefel	Mean	5614.696	5468.771204
	Standard Deviation (SD)	583.4996	446.447
	P-Value	0.241322	0
Penalty #1	Mean	18,595,594	11,690,879.79
	Standard Deviation (SD)	13,784,289	8870459
	P-Value	0.73373	3.81152E-73
Penalty #2	Mean	63,937,965	55,712,723.73
	Standard Deviation (SD)	24,464,971	25,818,606
	P-Value	0.307489	1.02433E-91
Rosenbrock	Mean	1,331.466	1062.02699
	Standard Deviation (SD)	691.616	508.3196
	P-Value	0.307489	1.1419E-203
Quartic	Mean	9.618467	8.716411017
	Standard Deviation (SD)	6.949806	5.086379
	P-Value	0.57075	9.6298E-180
Rastrigin	Mean	135.3346	131.0232107
	Standard Deviation (SD)	29.70814	17.31392
	P-Value	0.000246	0

Table 5. Performance comparison of ASCBBO on mutation operator

Name of the Function	Criteria	CBBO (Saremi, Mirjalili & Lewis, 2014)	ASCBBO
Sphere	Mean Standard Deviation (SD) P-Value	57.38914 18.31544 0.088973	50.1449926 17.44709 2.7128E-119
Ackley	Mean Standard Deviation (SD) P-Value	16.71692 0.909707 0.520523	16.4889305 0.444036 0
Griewank	Mean Standard Deviation (SD) P-Value	177.019 48.90111 0.037635	160.480161 41.94935 3.6301E-228
Fletcher	Mean Standard Deviation (SD) P-Value	802,456 263,524.6 0.021134	684040.4607 143144 2.083E-118
Schwefel	Mean Standard Deviation (SD) P-Value	5,792.544 677.7967 0.140465	5686.935398 400.0152 3.8178E-291
Penalty #1	Mean Standard Deviation (SD) P-Value	22,986,907 10,639,030 0.121225	13,494,022.35 6080759 3.09833E-61
Penalty #2	Mean Standard Deviation (SD) P-Value	64,692,549 30,294,479 0.57075	59643824.68 21092195 4.50373E-98
Rosenbrock	Mean Standard Deviation (SD) P-Value	1,378.675 655.9377 0.161972	1021.611419 403.1622 9.083E-137
Quartic	Mean Standard Deviation (SD) P-Value	11.30964 4.400924 0.241322	10.26638274 3.569843 6.6395E-267
Rastrigin	Mean Standard Deviation (SD) P-Value	77.96833 12.21388 0.57075	149.3794566 21.35098 0

Table 6. Performance comparison of GWO, SCA, ALO, GA and DE algorithms on CEC 2014 test suite

Criteria	F_n's	GWO	SCA	ALO	GA	DE
Mean	F1	19182560.98	344799637.4	36745224.63	325060465.3	413415603.7
SD		1634289.478	344799637.4	6728505.317	150130056.4	101727229.1
P-Value		3.66049E-58	2.097E-305	2.27658E-58	1.15518E-06	3.77609E-88
Best Value		18026943.81	308735840	31987452.89	218902484.4	341483590.1
Mean	F2	106497255.4	258967730	37690508.33	265040650.9	395816684.8
SD		0	0	0	0	0
P-Value		1.08637E-49	0.5	7.93186E-59	1.11826E-15	7.0177E-124
Best Value		106497255.4	258967730	37690508.33	265040650.9	395816684.8
Mean	F3	78602686.25	311450961.4	21456174.11	277242810.6	398201442.7
SD		31730057.75	65311605.67	8954463.125	123952216.2	19673665.33
P-Value		1.44955E-79	0	1.52242E-84	1.50701E-13	1.153E-182
Best Value		43725267.89	250994542.5	11144127.91	184793125.2	385962417.2
Mean	F4	23155981.89	398227090.1	24728929.87	109886137.7	486477111.8
SD		0	0	0	120430478.3	0
P-Value		7.46102E-36	4.01337E-80	2.3917E-48	4.94624E-30	3.6446E-138
Best Value		23155981.89	398227090.1	24728929.87	24728929.87	486477111.8
Mean	F5	30236109.49	272283861.6	29867995.33	299915987.4	421926579.8
SD		26829055	86184274.7	4224313.46	88761120.9	44526977.5
P-Value		0.63689855	0	0	0.29335765	0.00036235
Best Value		7517930	156021286	24382449.9	217403686.2	362787480
Mean	F6	65558965.12	372280262.9	36193407.86	347946851.4	454450366.1
SD		26275801.93	33920574.26	7075680.726	58123140.63	121434239.3
P-Value		0.016526431	0	0	0.255260992	0.000996497
Best Value		31448013.78	351312632.7	28175185.48	297678679.9	277683935.9
Mean	F7	38798267.35	362375662.3	31020496.82	412494075.5	508989497.7
SD		36446207.59	82496909.34	10440812.45	122748651.3	36702429.81
P-Value		0.01549549	0	1.36651E-84	1.45104E-18	3.4007E-130
Best Value		16773128.53	267871472.7	24421416.16	272983669.5	468229555.3
Mean	F8	92064101.26	301361308.7	27806185.87	251692757.7	426073341.2
SD		27585129.3	80726961.74	7936210.397	76949536.28	49593096.07
P-Value		1.7121E-119	0	1.7219E-100	2.5349E-18	3.7994E-225
Best Value		64626242.67	194131013.6	20215308.44	201219765.1	372667030.6
Mean	F9	33759495.51	287682281.9	32407103.99	340944716.4	404164883.2
SD		21840960.33	106119692.9	7937057.089	86848646.6	100695458
P-Value		9.7753E-195	0	1.6131E-166	5.31973E-18	0
Best Value		10090118.93	156021285.6	24382449.95	218005377.8	277683935.9
Mean	F10	50658045.2	359609904.9	32162399.94	383790226.6	504904159.7
SD		38054802.87	67585188.39	8825501.719	115500929.4	31061318.65
P-Value		1.3186E-117	0	1.8871E-112	1.45025E-21	3.5832E-166
Best Value		16773128.53	267871472.7	24421416.16	272983669.5	468229555.3
Mean	F11	85957097.24	288312248.1	24820586.68	304244587.6	431683252.1
SD		36836888.01	77790816.23	6789542.008	110285090.7	58978580.02
P-Value		3.1885E-128	0	4.8847E-106	7.92746E-18	6.4205E-231
Best Value		40198226.59	194131013.6	20215308.44	201219765.1	372667030.6
Mean	F12	38386823.52	341143347	26178497.54	172302412	349352644.9
SD		18440532.33	103261364.3	10573734.22	93183422.59	95270338.77
P-Value		1.05715E-58	0	7.9729E-144	2.76862E-28	9.8433E-253
Best Value		23601062.25	231220358.3	16191941.26	7105940.56	258258757.2
Mean	F13	85533779.63	299214208.9	22165048.21	279205562.1	358770541.6
SD		65486951.33	77806468.38	9312152.925	66847690.19	49522989.25
P-Value		5.3242E-104	0	2.7212E-100	1.0131E-14	2.9977E-227
Best Value		25454062.19	212170539.7	10146554.65	244959239.3	301109701.5
Mean	F14	42106126.06	412616910	28240536.44	184242003.7	373820106.1
SD		34778442.87	104124729.6	6921833.111	136842993.8	36441624.75
P-Value		6.278E-134	0	9.1913E-100	1.50263E-44	2.6136E-280
Best Value		18065763.12	264136501.4	24558814.18	12001742.12	347979254.3
Mean	F15	52311091.57	373394793.1	33514420.4	326770077.5	411001868.4
SD		21589759.35	99777594.86	9500126.97	138325062.2	40867633.63
P-Value		2.87306E-97	0	1.466E-119	1.12175E-16	2.9247E-177
Best Value		28290051.43	288350619.3	21470634.55	182766458.3	357361676.4

continued on next page

Table 6. Continued

Criteria	F_n's	GWO	SCA	ALO	GA	DE
Mean SD P-Value Best Value	F16	92068497.45 64261783.93 2.239E-108 30226702.53	472850903.5 120909437.6 0 352481422.8	30601401.58 10304706.14 6.7248E-124 16302551.27	427074531.3 109503838.9 7.59078E-28 314957781.2	407214885.9 52649178.12 0 314777995.7
Mean SD P-Value Best Value	F17	90978158.14 97170804.05 1.4422E-99 19445735.05	411101836 133106990.4 0 282933253	38577894.23 8756314.761 1.22937E-89 29995242.01	371047709.7 131573039.5 1.54419E-10 236028512.2	431144746 16207649.75 2.1978E-191 415277763.2
Mean SD P-Value Best Value	F18	53189723.43 30839178.83 4.32731E-80 18026943.81	346722064.7 35221868.93 0 308735840	36276080.12 6719571.732 1.19544E-83 28696521.5	404730981.1 69236836.84 1.12861E-14 326160759.2	348797777 27394820.71 1.3457E-197 325802418.3
Mean SD P-Value Best Value	F19	46218374.45 23070217.38 3.5336E-104 20338178.15	326676176.1 58379900.3 0 264854769.6	32817860.06 1375388.948 5.1342E-73 31987452.89	218103849.5 754235.7175 3.36826E-10 217403686.2	444636491.6 70883644.63 4.859E-159 362787479.8
Mean SD P-Value Best Value	F20	40268830.76 31831306.07 3.1582E-209 10090118.93	304973854.5 108487661.3 0 156021285.6	33112592.34 8054466.281 3.9519E-157 24382449.95	356879376.8 62568066.15 5.04237E-19 280204564.2	430137016.4 104046553 3.8428E-291 277683935.9
Mean SD P-Value Best Value	F21	61553764.42 54376477.32 3.70721E-93 16773128.53	320314500.1 107766996.3 0 194131013.6	28319199.72 10092657.41 2.9063E-107 20215308.44	400958424.2 102845057.9 7.01292E-20 272983669.5	482047506.3 61656542.07 3.9001E-188 401221532
Mean SD P-Value Best Value	F22	71336044.44 27436897.93 1.9706E-140 40198226.59	319705993 56246896.25 0 282114081.7	26355679.42 7416721.822 4.49493E-84 21695671.29	283542293.3 125190622.3 4.64907E-16 201219765.1	441837158.9 67816652.98 1.2288E-176 372667030.6
Mean SD P-Value Best Value	F23	43449356.13 23071031.75 3.72553E-51 23601062.25	346725494.8 104386839.1 8.1454E-300 231220358.3	24514071.49 11514391.47 5.84899E-88 16191941.26	207890117.7 15903623.77 8.91914E-14 196467293.5	372127271.7 113870824.4 8.3882E-137 258258757.2
Mean SD P-Value Best Value	F24	85533779.63 65486951.33 5.3242E-104 25454062.19	299214208.9 77806468.38 0 212170539.7	22165048.21 9312152.925 2.7212E-100 10146554.65	279205562.1 66847690.19 1.0131E-14 244959239.3	358770541.6 49522989.25 2.9977E-227 301109701.5
Mean SD P-Value Best Value	F25	64321517.6 40593900.26 1.97154E-75 35617295.44	344657162.5 113873411 0 264136501.4	31802081.84 9641992.198 2.85034E-49 24984163.77	289669516.2 164110848.2 1.14293E-08 173625622.6	387871346.6 56415938.02 5.7914E-137 347979254.3
Mean SD P-Value Best Value	F26	31147895.49 19583195.34 6.28922E-75 18065763.12	416501311.4 113398666 0 288350619.3	23609538.88 1856239.822 1.46712E-83 21470634.55	280027357.9 69979375.8 6.59253E-14 206099053.5	358966469.2 2768716.562 7.5883E-188 357361676.4
Mean SD P-Value Best Value	F27	63646048.72 23718235.77 1.02524E-72 46874723.37	345509298.8 35356502.07 3.1436E-293 320508476.4	40568596.78 4681796.076 3.41306E-56 37258067.03	417786214.2 136566369.7 1.77282E-09 321219208.1	440930638.2 17409833.75 4.48941E-73 428620026.6
Mean SD P-Value Best Value	F28	89938418.95 65301200.03 1.17784E-50 28290051.43	553865227.5 70689665.01 4.5562E-270 511905945	25141708.69 7884460.024 2.83205E-91 16302551.27	384871344.2 181407601.1 3.98872E-15 182766458.3	386657999.8 64748523.88 1.3707E-228 314777995.7
Mean SD P-Value Best Value	F29	94571813.96 93325878.08 4.32536E-67 30226702.53	434284559.3 102058299.4 8.3049E-228 352481422.8	36305026.95 5598877.866 2.7277E-82 29995242.01	397357466 93440398.08 7.79956E-13 314957781.2	427729109.7 17448836.27 3.5403E-172 415277763.2
Mean SD P-Value Best Value	F30	53662653.85 30030606 1.1722E-136 19445735.05	338121202.4 49423146.59 0 282933253	38274450.95 9405798.902 2.94087E-81 28696521.5	339667669.8 111010614.2 2.08155E-12 236028512.2	378464461.3 52343573.13 2.1724E-237 325802418.3

Table 7. Performance comparison of ACO, GSA, ASCBBO and SCBBO on CEC 2014 test problems

Criteria	F_n's	ACO	GSA	ASCBBO	SCBBO
Mean	F1	1118153230	11937855723	15545748.84	17331986.44
SD		381805571.1	1065982215	5668303.702	2506811.25
P-Value		1.3219E-204	0.5	6.06145E-61	1.39528E-29
Best Value		848175921.3	11184092470	11537652.86	15559403.21
Mean	F2	1187796885	10793061835	27167185.9	10776227.62
SD		0	0	0	0
P-Value		7.2024E-272	1	1.21664E-63	3.54011E-22
Best Value		1187796885	10793061835	27167185.9	10776227.62
Mean	F3	1191138207	10404035657	25867803.77	12358185.35
SD		172434492.2	2771844256	3144848.27	6102520.877
P-Value		0	0.5	1.1415E-118	3.31609E-45
Best Value		1003605355	8311562496	22292698.4	8056865.491
Mean	F4	1311905424	8746848523	12316914.27	10040023.07
SD		0	0	0	0
P-Value		2.29594E-94	0	5.03855E-61	5.72176E-28
Best Value		1311905424	8746848523	12316914.27	10040023.07
Mean	F5	1043181055	8373429232	20331326.74	13908371.54
SD		299660809.1	4925711646	4661827.306	2635470.768
P-Value		2.85107E-22	0.500000313	4.40135E-07	0.00255038
Best Value		547780006	2563595031	20521171.8	13527839.18
Mean	F6	1234734464	14981779398	24009235.51	21402200.97
SD		160120928.8	10743447321	7840972.761	8176446.668
P-Value		4.28846E-11	0.5	3.34467E-10	0.026136442
Best Value		1037691981	6873457609	16553179.82	13934948.88
Mean	F7	1357587582	5553237878	28710269.04	15688832.81
SD		93937754.32	665585370.6	626335.4764	7189161.509
P-Value		4.3544E-229	0.5	2.83334E-93	3.84619E-37
Best Value		1257364300	4802300245	27991957.78	8361832.406
Mean	F8	1039821214	5459806647	22362167.6	14464416.77
SD		210993048.1	2231386040	3474443.513	4236801.357
P-Value		0	0.5	2.2876E-114	3.38233E-49
Best Value		838827867.9	2836801818	17703111.18	9759022.651
Mean	F9	1040125812	11353659989	1390688626	21499023.79
SD		327294797.8	11272493449	3064964860	11693373.56
P-Value		0	0.5	2.62209E-16	4.4594E-101
Best Value		547780006	2563591480	14665185.15	9905264.382
Mean	F10	1327109228	6944785680	27084362.19	16592818.7
SD		97972384.65	2835658135	3291781.135	6142051.022
P-Value		8.3903E-280	0.5	7.7937E-129	6.80633E-58
Best Value		1235674165	4802300245	22206641.66	8361832.406
Mean	F11	1036230777	4840947332	22877719.61	12401375.45
SD		205831084.6	1821692469	2594154.483	4801953.804
P-Value		0	0.5	1.4012E-123	4.1315E-50
Best Value		838827867.9	2836801818	19765319.23	8378279.964
Mean	F12	1135053783	4833788231	15470307.93	9563354.437
SD		191833605.5	8376207874	4242995.689	2351427.99
P-Value		0	0.5	1.9514E-113	1.61057E-75
Best Value		925161638.5	171333976.8	10944360.19	7105940.56
Mean	F13	1120054168	6962503268	24546729.88	2401827.94
SD		110289283.3	4942727716	7482026.599	2401827.94
P-Value		0	0.5	5.6399E-120	5.03904E-69
Best Value		1037158174	1485128199	15832809.18	11276776.84
Mean	F14	1164472822	7286903474	20408402.53	15062632.29
SD		115845116.7	3263910120	10601253.4	2155051.677
P-Value		0	0.5	4.0729E-108	1.82859E-67
Best Value		1012476900	2567200505	9170735.569	12001742.12
Mean	F15	1442801218	11089860883	23700359.66	15418602.59
SD		247289417.7	4746103295	8275476.573	3174520.212
P-Value		0	0.5	3.86746E-96	6.64759E-59
Best Value		1089635478	5659847532	15493787.77	11578302.03

continued on next page

Table 7. Continued

Criteria	F_n's	ACO	GSA	ASCBBO	SCBBO
Mean	F16	909911166.7	28720156835	20803503.83	17183643.71
SD		69793333.4	10739099605	5238569.75	3658935.783
P-Value		0	0.5	5.8489E-117	2.037E-78
Best Value		823134475.2	14914085257	16781720.34	14453502.7
Mean	F17	228898664.1	7572499057	18542494.59	14371660.71
SD		228898664.1	5507828061	6691233.931	3707636.368
P-Value		0	0.5	1.50302E-60	2.59881E-35
Best Value		990711125.7	4094171147	11026020.9	10174213.2
Mean	F18	939526692.6	11349802839	21369095.08	15238567.08
SD		128324765.8	6570539205	3219300.392	4812294.805
P-Value		0	0.5	1.65496E-95	4.78247E-29
Best Value		848175921.3	4211930063	19467352.85	10273882.21
Mean	F19	1068614183	8094412370	14635316.4	15213426.44
SD		454910874.3	2805912796	3082837.687	4760542.115
P-Value		9.9066E-277	0.5	2.43432E-75	6.23489E-52
Best Value		547780006	5704850901	11537652.86	9905264.382
Mean	F20	1177704644	12436575625	24519493.19	19151820.18
SD		180057372.5	10846182772	6985913.2	8105914.762
P-Value		0	0.5	9.8014E-152	5.26828E-89
Best Value		972959618.2	2563591480	16553179.82	13527839.18
Mean	F21	1239247896	4874128863	27067496.26	14206380.27
SD		248797093.3	1462905377	3325107.575	6576221.63
P-Value		6.4725E-254	0.5	2.688E-125	4.08007E-45
Best Value		884228835.4	2836801818	22139177.92	8361832.406
Mean	F22	1086898090	5508995837	23123900.17	13282159.71
SD		219423319.1	1516612129	3119427.352	5471147.501
P-Value		0	0.5	4.67667E-91	1.26256E-42
Best Value		838827867.9	4376160057	19765319.23	8378279.964
Mean	F23	1155823850	7315309905	15710323.17	9153785.457
SD		200088979.9	10786356288	4293607.723	2605247.438
P-Value		1.6856E-182	0.5	3.48833E-70	1.67011E-45
Best Value		925161638.5	171333976.8	10944360.19	7105940.56
Mean	F24	1120054168	6962503268	24546729.88	13386421.46
SD		110289283.3	4942727716	7482026.599	2401827.94
P-Value		0	0.5	5.6399E-120	1.77802E-60
Best Value		1037158174	1485128199	15832809.18	11276776.84
Mean	F25	1142869513	9242949253	21031548.88	14309906.27
SD		184403001.6	1174421274	10500970.43	3264237.048
P-Value		0	0.5	2.60451E-48	2.61314E-46
Best Value		1012476900	8412508006	13606241.49	12001742.12
Mean	F26	1153929247	5440520974	21872189.81	16843799.59
SD		72765127.11	2770176740	11213113.92	1917975.821
P-Value		0	0.5	8.25947E-85	3.33118E-37
Best Value		1089635478	2567200505	9170735.569	15104333.06
Mean	F27	1611131561	14156157231	26630796.9	15597713.09
SD		42278866.12	4335144765	10743625.75	1815430.601
P-Value		1.2965E-141	0.5	3.24213E-56	2.80727E-27
Best Value		1581235888	11090746971	19033906.28	14314009.81
Mean	F28	1088075001	21646843273	16552678.33	13553647.74
SD		331137329.4	15745337898	964976.1777	1712952.124
P-Value		0	0.5	6.28332E-50	2.58569E-45
Best Value		823134475.2	10387281537	15493787.77	11578302.03
Mean	F29	1001523702	14442504152	20470528.53	18043935.43
SD		125852410.5	10011927316	8288707.659	2821494.468
P-Value		0	0.5	5.90716E-75	7.71395E-44
Best Value		881426422.7	4700578956	11026020.9	15740560.38
Mean	F30	1136321458	8483986896	21768371.46	13443503.74
SD		280570355	7501632774	2944112.809	5576484.099
P-Value		1.6532E-278	0.5	1.75406E-96	1.62648E-32
Best Value		884164842.8	4094171147	19467352.85	10174213.2

Figure 3a. Convergence curves for simple BBO operator

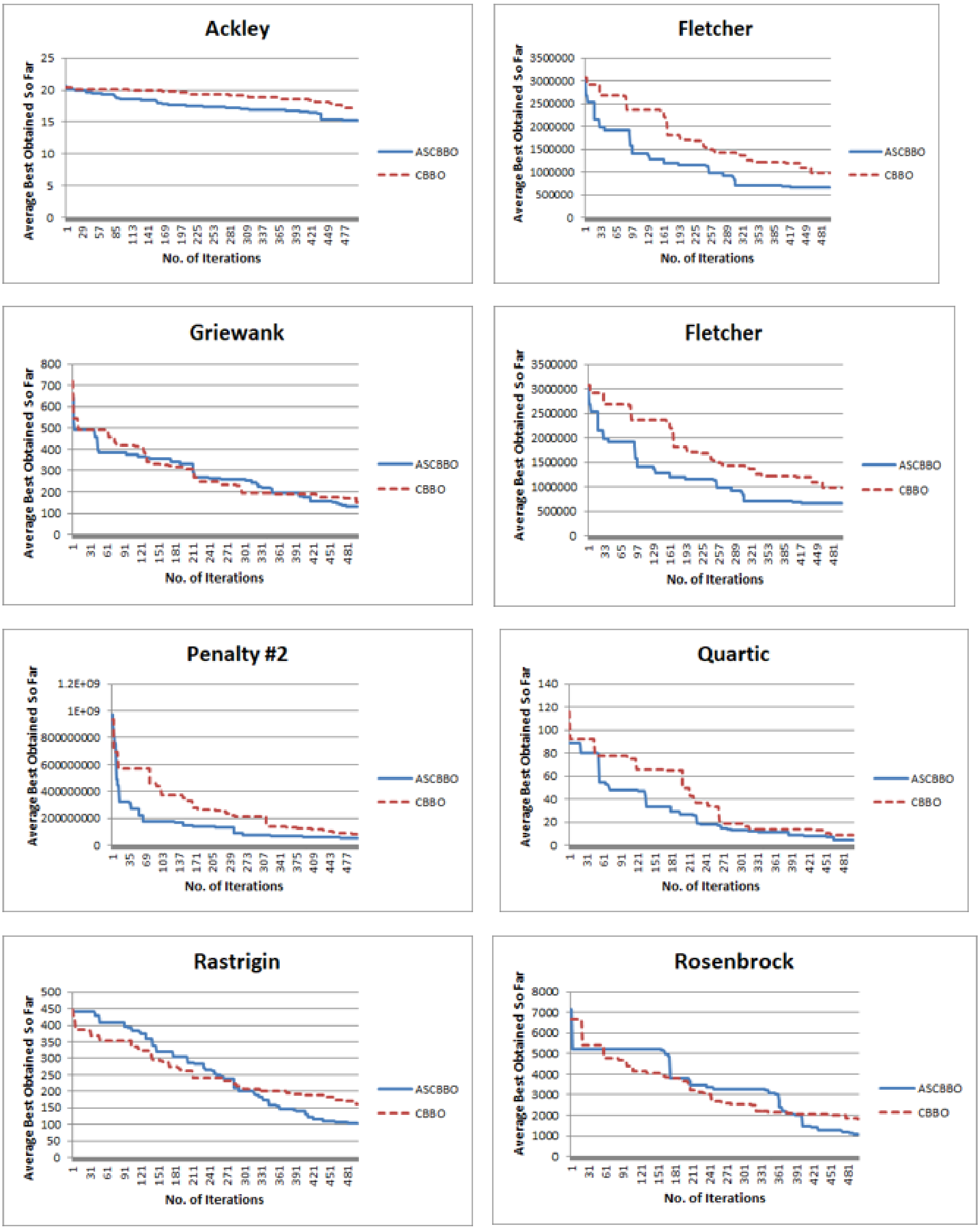

Figure 3b. Convergence curves for simple BBO operator

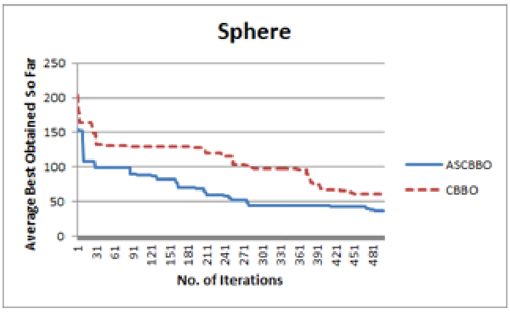

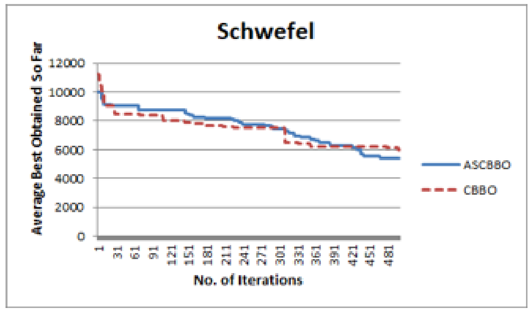

Figure 4a. Convergence curves for mutation operator on CBBO and ASCBBO

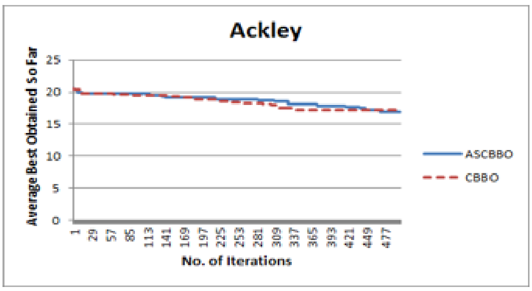

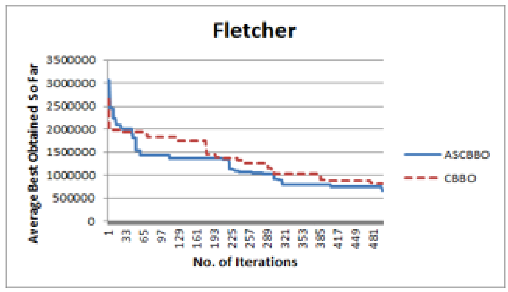

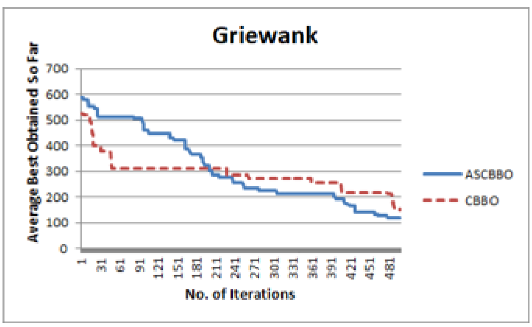

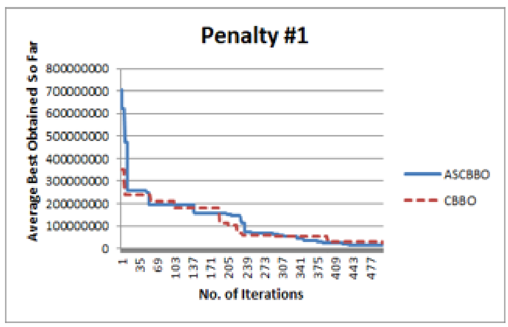

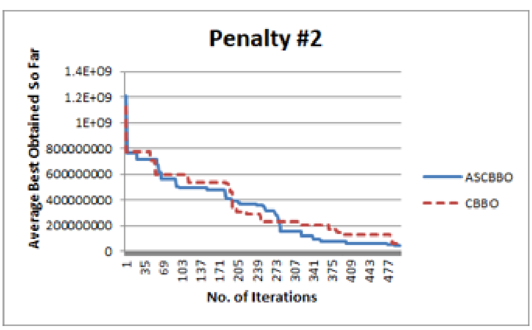

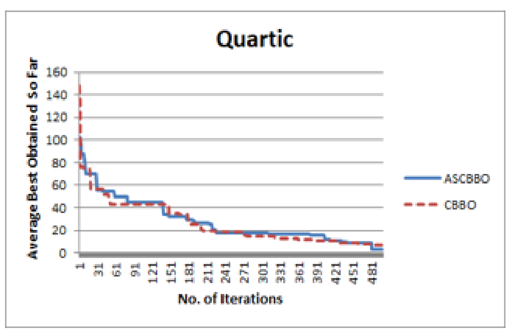

Figure 4b.

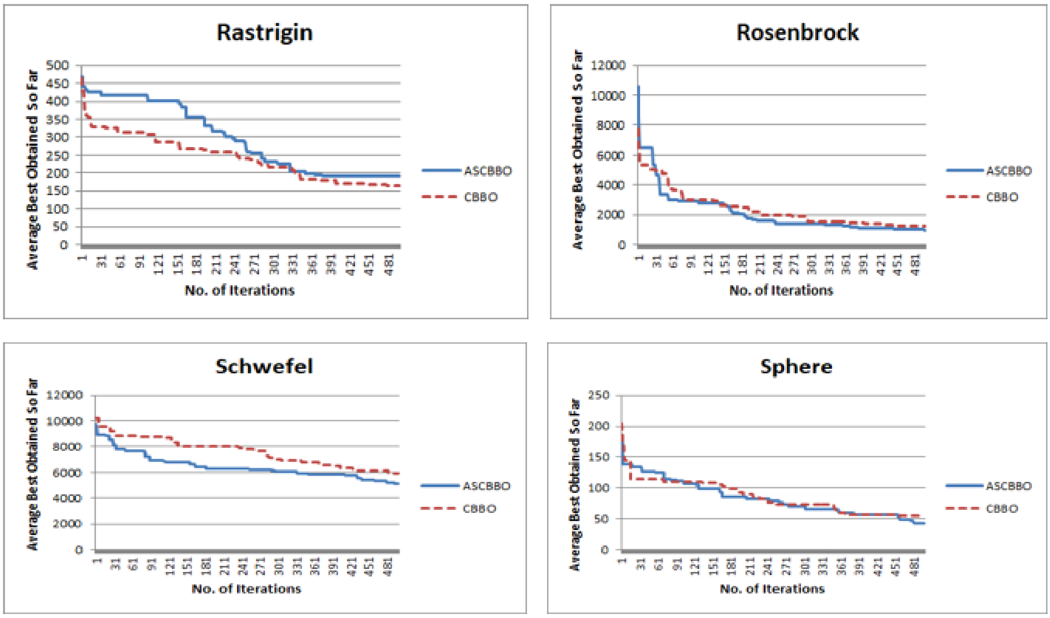

Figure 5a. Convergence curves for selection and migration operator combined on GWO, SCA, ALO, GA, DE, ACO, GSA, ASCBBO and SCBBO

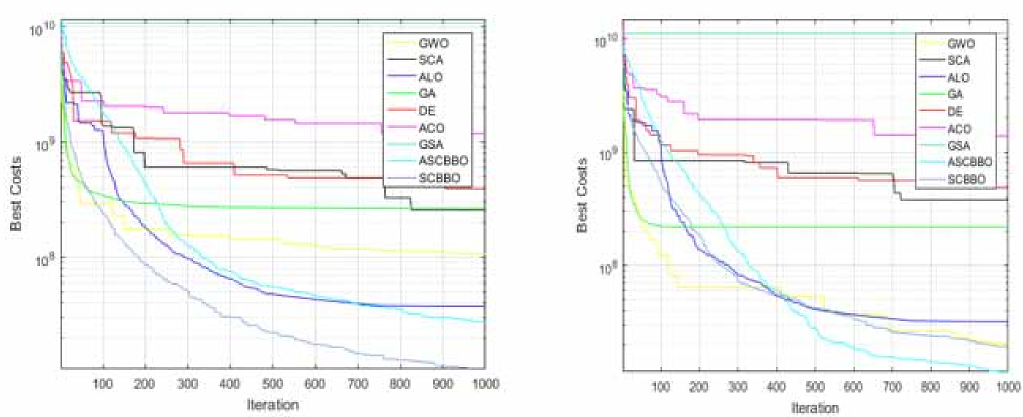

F1 F2

Figure 5b. Convergence curves for selection and migration operator combined on GWO, SCA, ALO, GA, DE, ACO, GSA, ASCBBO and SCBBO

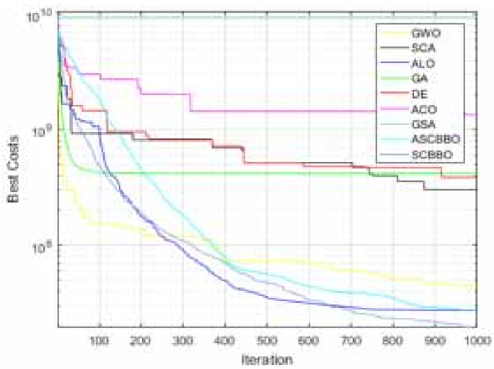

F3

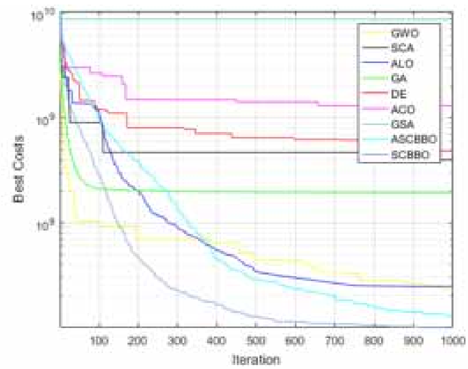

F4

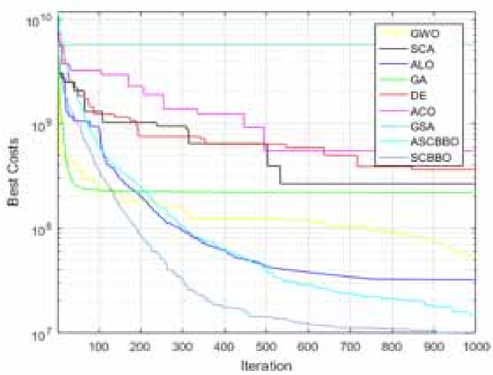

F5

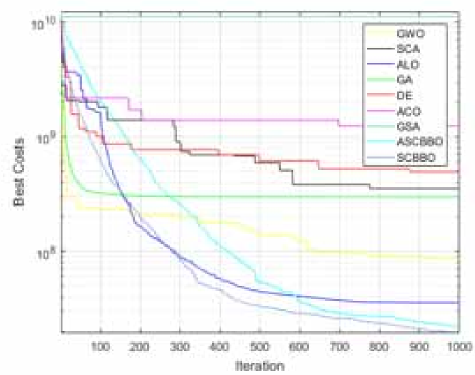

F6

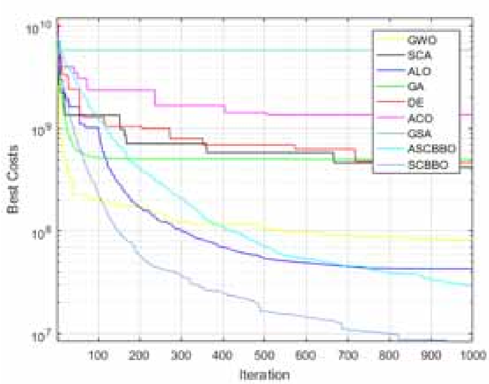

F7

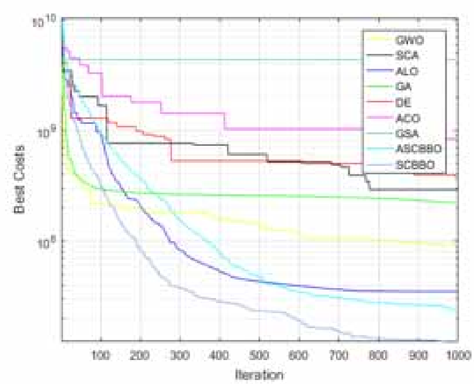

F8

Figure 5c. Convergence curves for selection and migration operator combined on GWO, SCA, ALO, GA, DE, ACO, GSA, ASCBBO and SCBBO

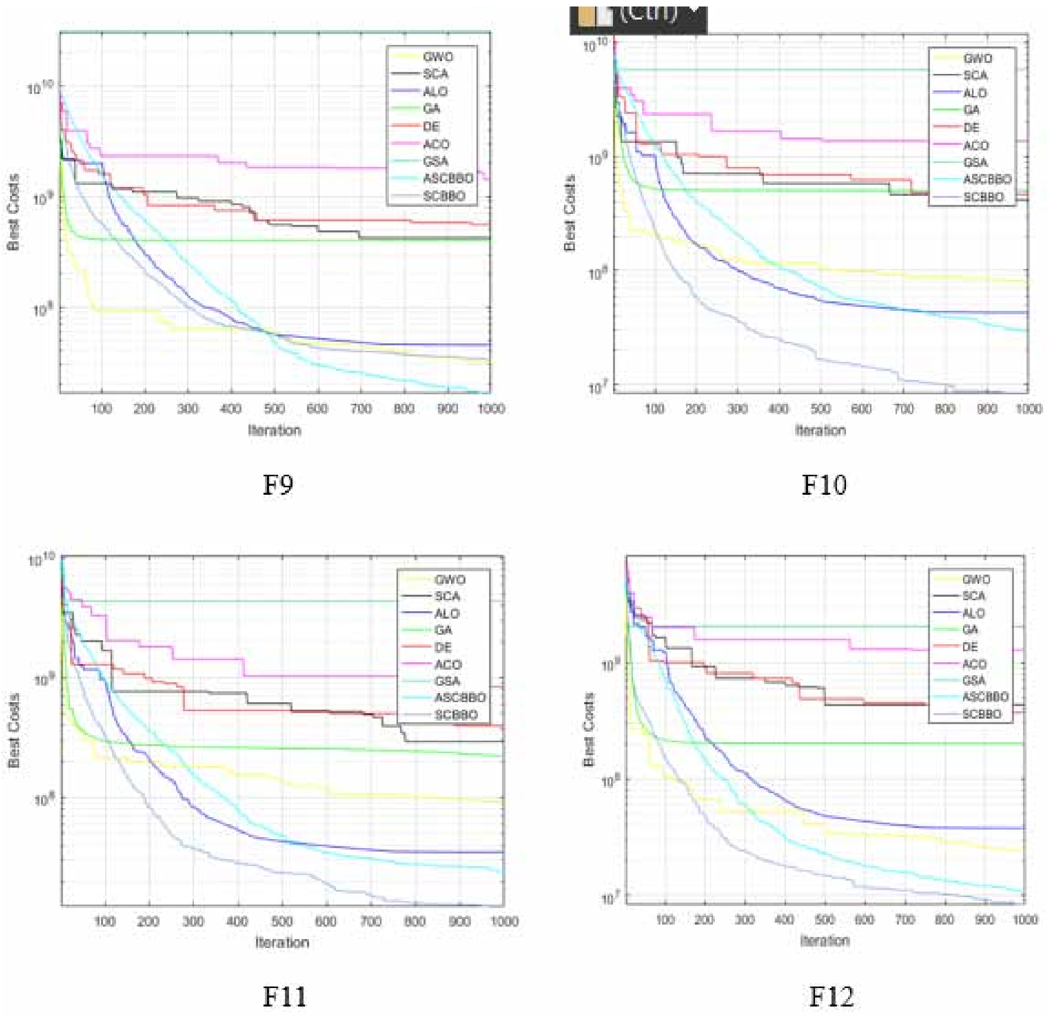

Figure 5d. Convergence curves for selection and migration operator combined on GWO, SCA, ALO, GA, DE, ACO, GSA, ASCBBO and SCBBO

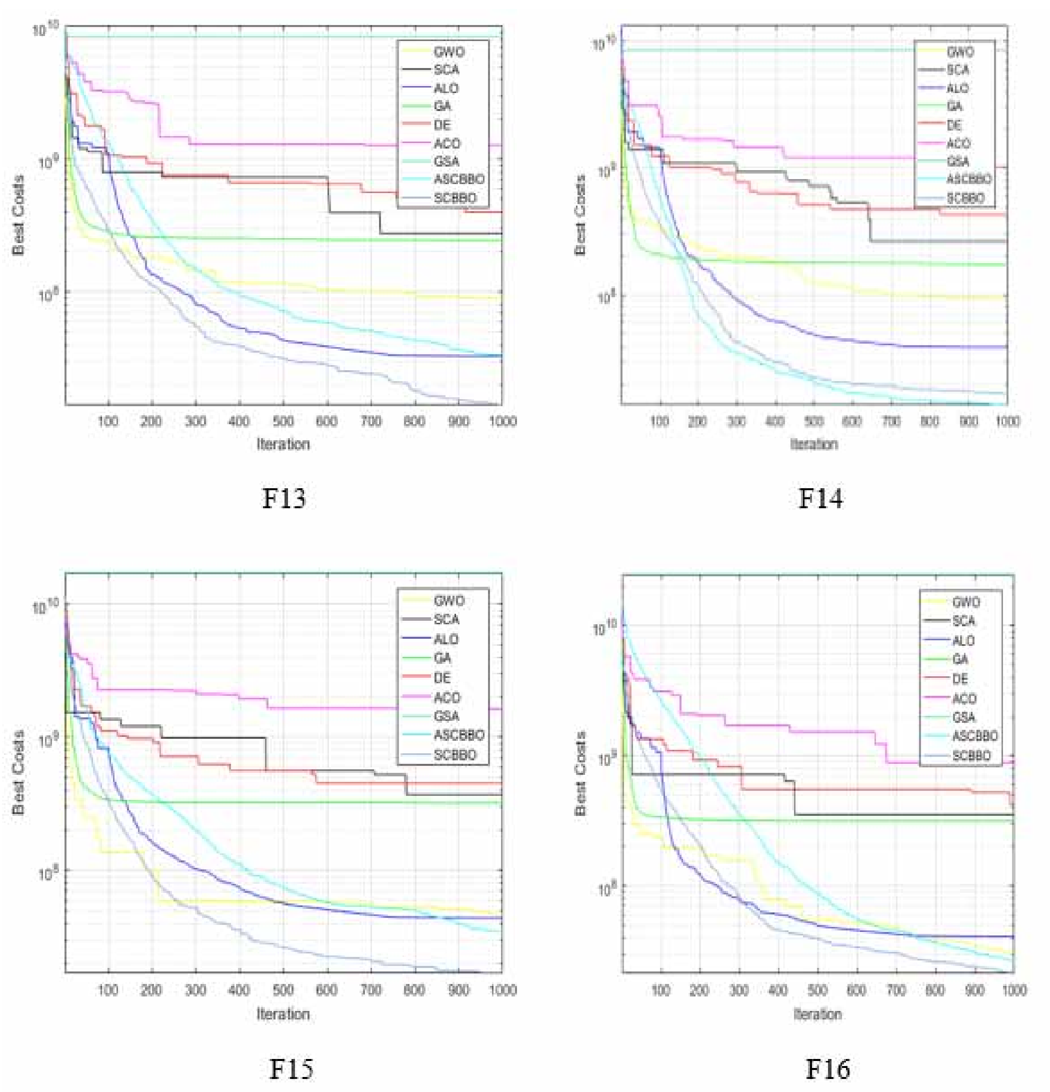

Figure 5e. Convergence curves for selection and migration operator combined on GWO, SCA, ALO, GA, DE, ACO, GSA, ASCBBO and SCBBO

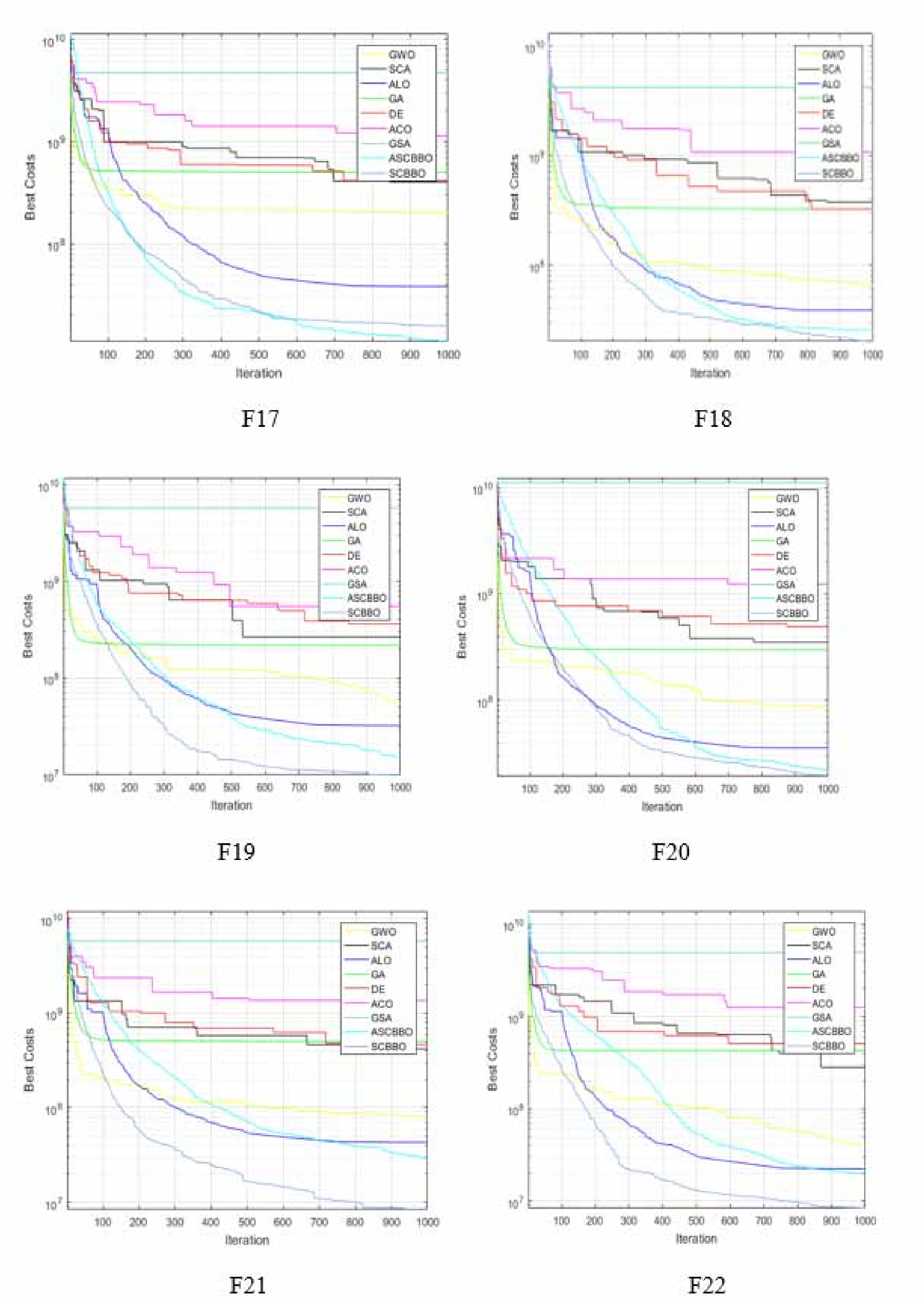

Figure 5f. Convergence curves for selection and migration operator combined on GWO, SCA, ALO, GA, DE, ACO, GSA, ASCBBO and SCBBO

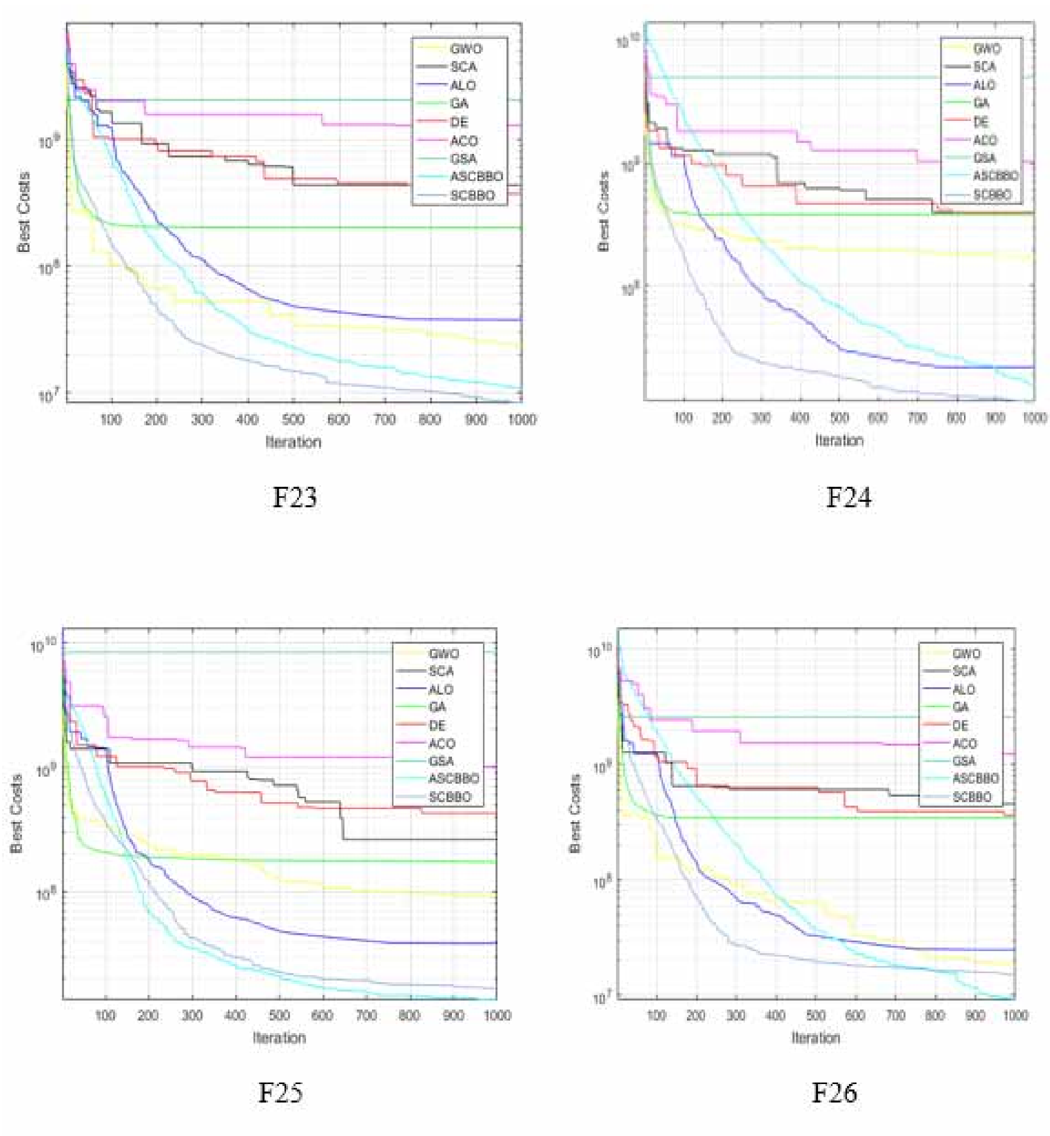

Figure 5g. Convergence curves for selection and migration operator combined on GWO, SCA, ALO, GA, DE, ACO, GSA, ASCBBO and SCBBO

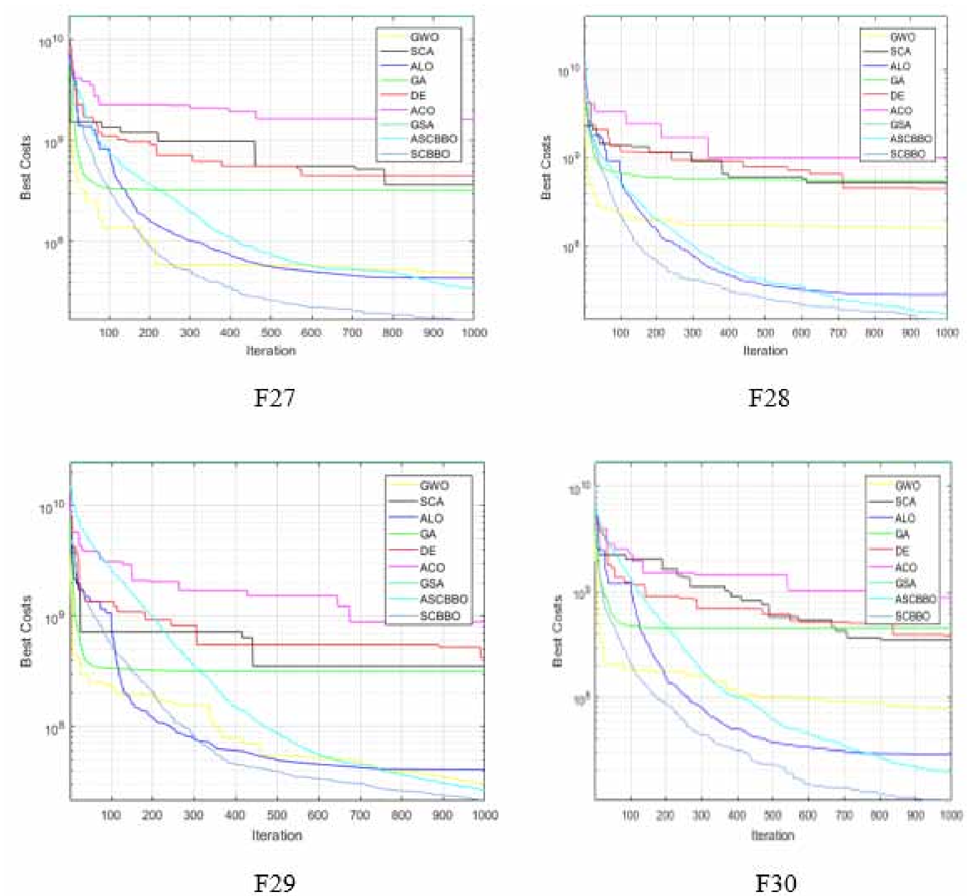

Figure 6a. Box plot graphs for selection and migration operator combined on GWO, SCA, ALO, GA, DE, ACO, GSA, ASCBBO and SCBBO

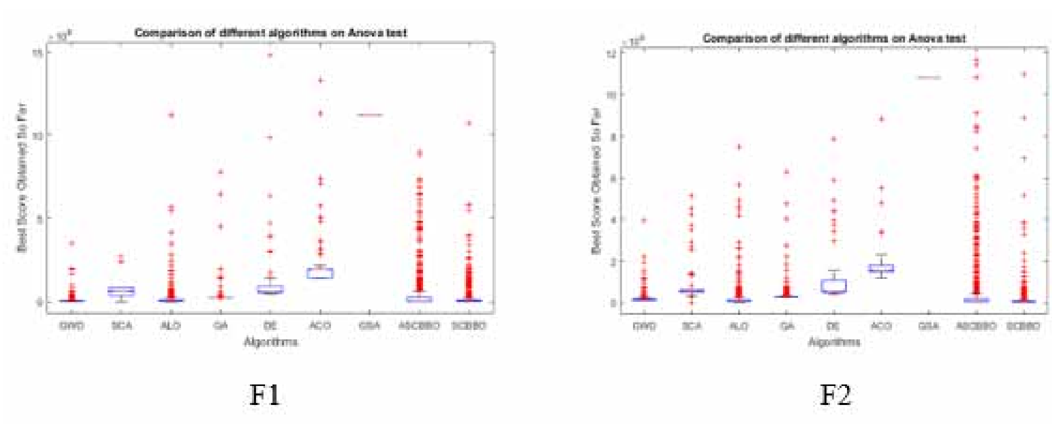

Figure 6b. Box plot graphs for selection and migration operator combined on GWO, SCA, ALO, GA, DE, ACO, GSA, ASCBBO and SCBBO

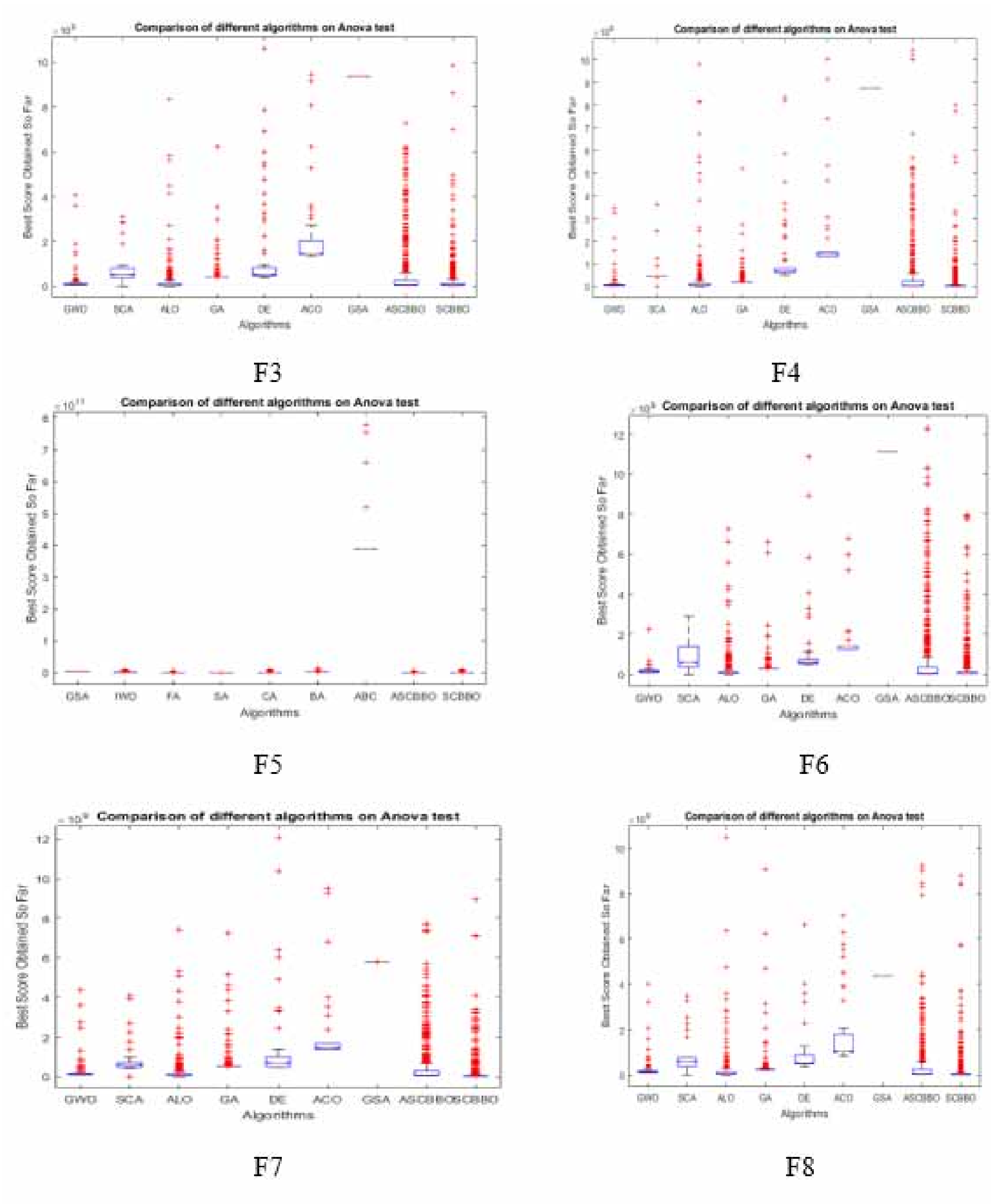

Figure 6c. Box plot graphs for selection and migration operator combined on GWO, SCA, ALO, GA, DE, ACO, GSA, ASCBBO and SCBBO

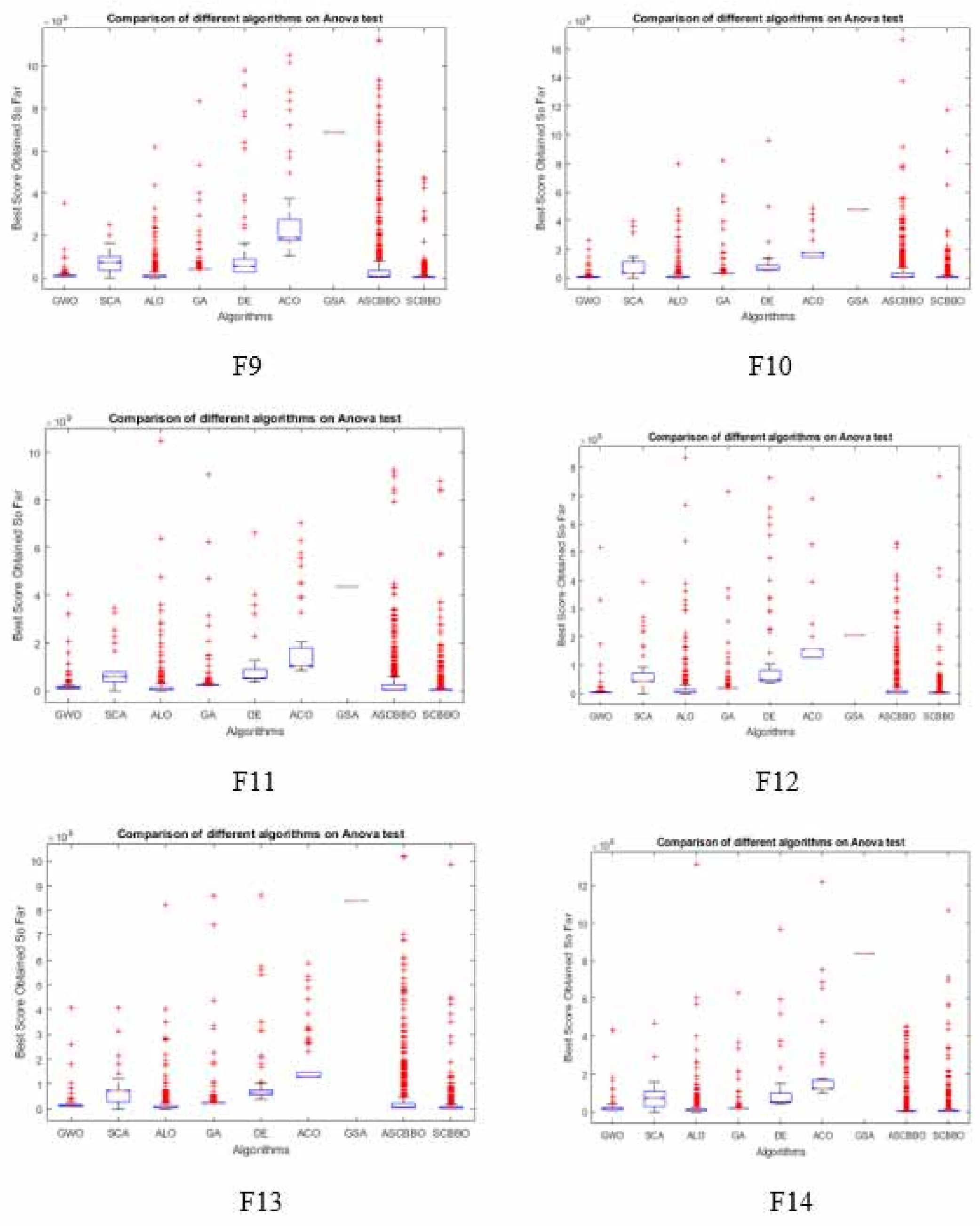

Figure 6d. Box plot graphs for selection and migration operator combined on GWO, SCA, ALO, GA, DE, ACO, GSA, ASCBBO and SCBBO

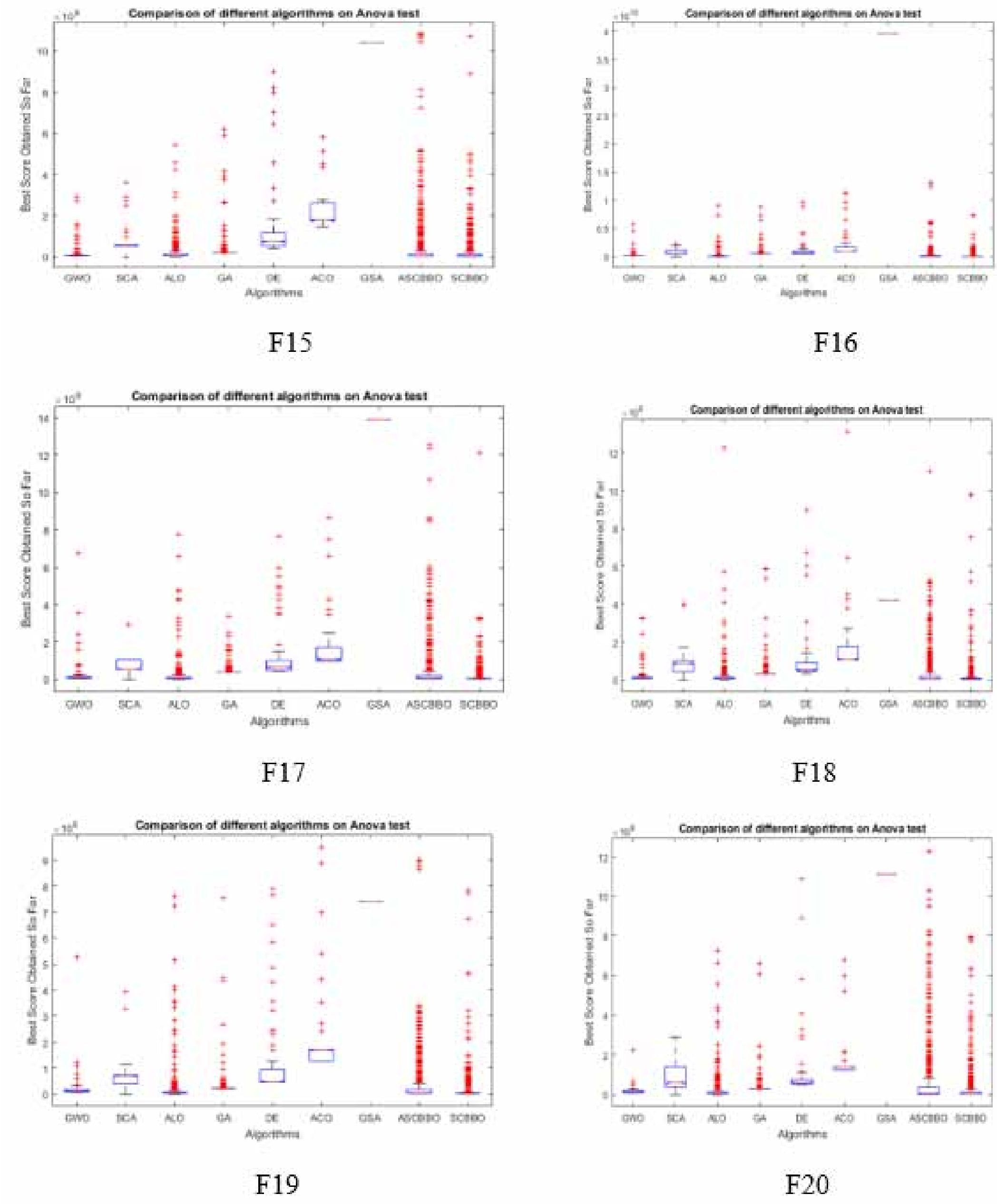

Figure 6e. Box plot graphs for selection and migration operator combined on GWO, SCA, ALO, GA, DE, ACO, GSA, ASCBBO and SCBBO

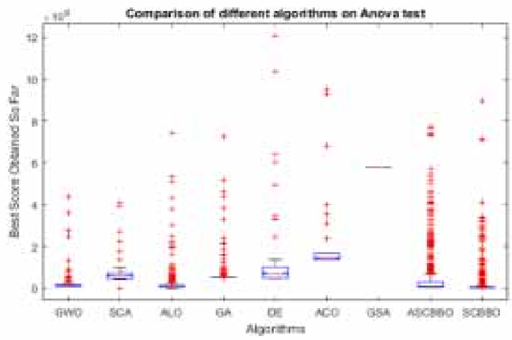

F21

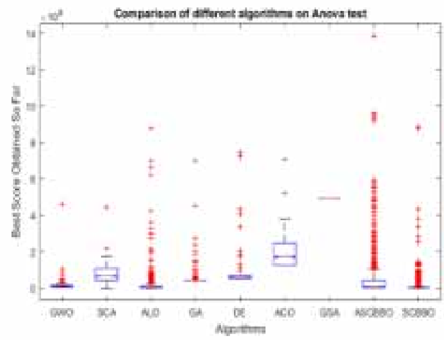

F22

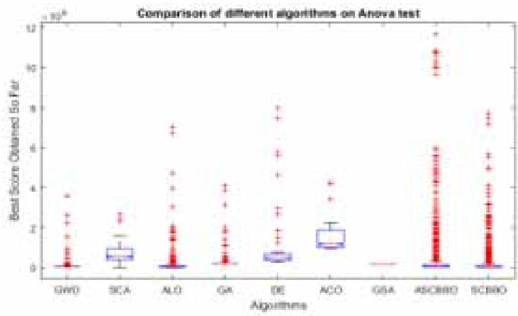

F23

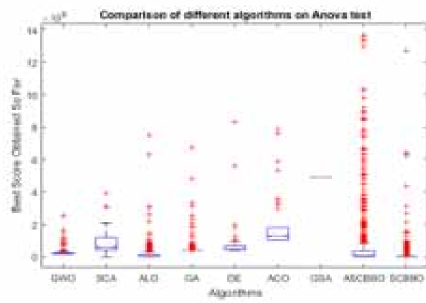

F24

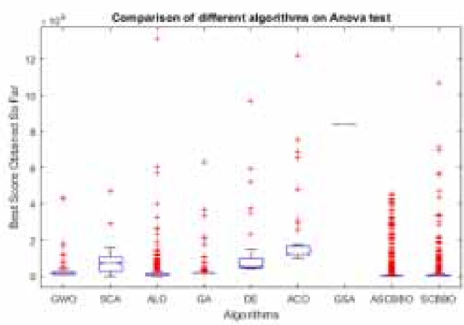

F25

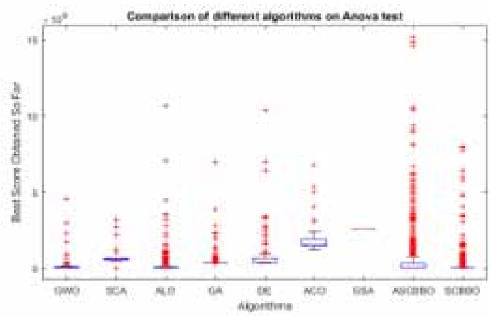

F26

Figure 6f. Box plot graphs for selection and migration operator combined on GWO, SCA, ALO, GA, DE, ACO, GSA, ASCBBO and SCBBO

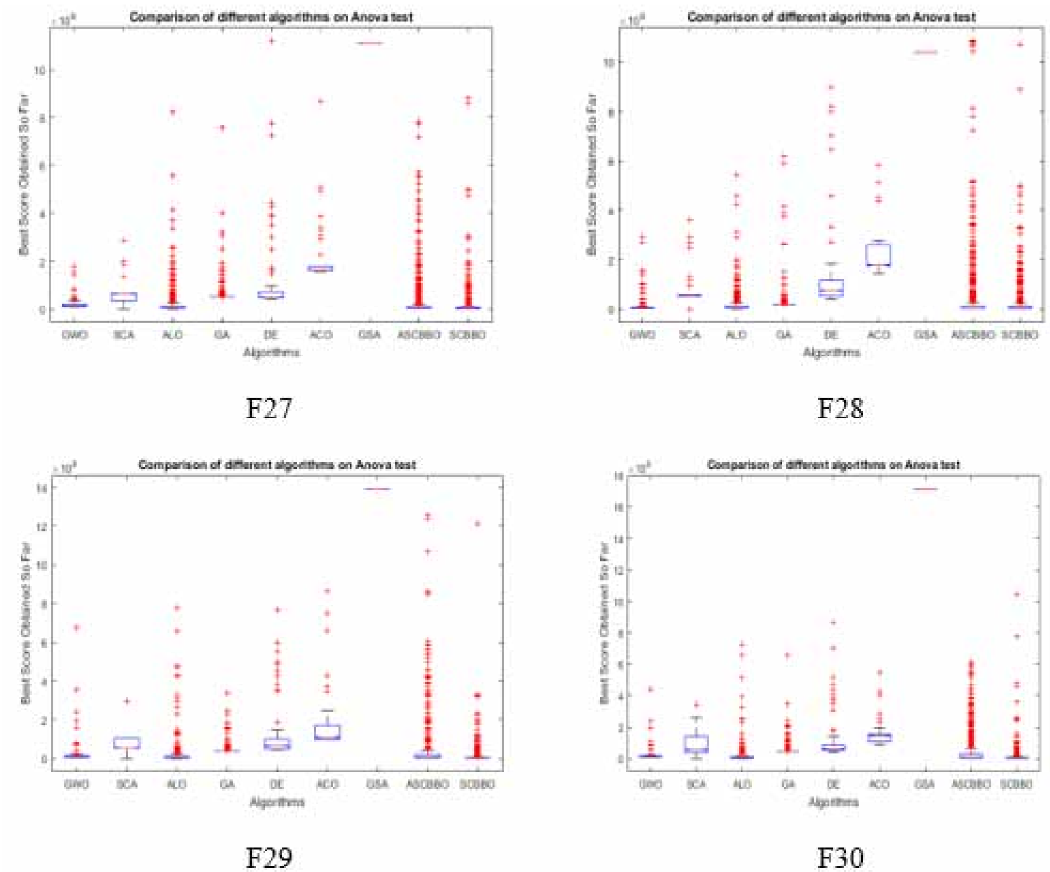

REFERENCES

Alatas, B. (2010a). Chaotic bee colony algorithms for global numerical optimization. *Expert Systems with Applications*, *37*(8), 5682–5687. doi:10.1016/j.eswa.2010.02.042

Alatas, B. (2010b). Chaotic harmony search algorithms. *Applied Mathematics and Computation*, *216*(9), 2687–2699. doi:10.1016/j.amc.2010.03.114

Alatas, B., Akin, E., & Ozer, A. (2009). Chaos embedded particle swarm optimization algorithms. *Chaos, Solitons, and Fractals*, *40*(4), 1715–1734. doi:10.1016/j.chaos.2007.09.063

Arslan, H., & Toz, M. (2019). Data clustering based on fuzzy c-means and chaotic whale optimization algorithms. *Sigma*, *37*(4), 1107–1128.

Arul, R., Ravi, G., & Velusami, S. (2013). An improved harmony search algorithm to solve economic load dispatch problems with generator constraints. *Electrical Engineering*, *96*(1), 55–63. doi:10.1007/s00202-012-0276-0

Ashish. (2014). *Fixed-point Iterative Procedure in Fractal and Chaos and the Stability of Functional Equations* (PhD). Maharishi Dayanand University, Rohtak, India.

Bejinariu, S. I., Costin, H., Rotaru, F., & Luca, R. (2019). *Data clustering by nature-inspired algorithms and chaotic maps. In 2019 E-Health and Bioengineering Conference (EHB)*. IEEE.

Bouyer, A., & Farajzadeh, N. (2015). An optimized K-harmonic means algorithm combined with modified particle swarm optimization and Cuckoo search algorithm. *Journal of Intelligent Systems*, *29*(1), 1–18. doi:10.1515/jisys-2015-0009

Danca, M., Fečkan, M., & Romera, M. (2014). Generalized form of Parrondo's paradoxical game with applications to chaos control. *International Journal of Bifurcation and Chaos in Applied Sciences and Engineering*, *24*(01), 1450008. doi:10.1142/S0218127414500084

Danca, M., & Tang, W. (2016). Parrondo's paradox for chaos control and anticontrol of fractional-order systems. *Chinese Physics B*, *25*(1), 010505. doi:10.1088/1674-1056/25/1/010505

Derrac, J., García, S., Molina, D., & Herrera, F. (2011). A practical tutorial on the use of nonparametric statistical tests as a methodology for comparing evolutionary and swarm intelligence algorithms. *Swarm and Evolutionary Computation*, *1*(1), 3–18. doi:10.1016/j.swevo.2011.02.002

Dhanusha, C., & Kumar, A. S. (2021). Deep recurrent Q reinforcement learning model to predict the alzheimer disease using smart home sensor data. *IOP Conference Series. Materials Science and Engineering*, *1074*(1), 012014. doi:10.1088/1757-899X/1074/1/012014

dos Santos Coelho, L., & Mariani, V. C. (2008). Use of chaotic sequences in a biologically inspired algorithm for engineering design optimization. *Expert Systems with Applications*, *34*(3), 1905–1913. doi:10.1016/j.eswa.2007.02.002

Du, D., Simon, D., & Ergezer, M. (2009). Biogeography-based optimization combined with evolutionary strategy and immigration refusal. In *2009 IEEE International Conference on Systems, Man and Cybernetics* (pp. 997-1002). IEEE. doi:10.1109/ICSMC.2009.5346055

Fang, U., Li, J., Lu, X., Ali, M., Gao, L., & Xiang, Y. (2021). Chaotic-to-fine clustering for unlabeled plant disease images. arXiv preprint arXiv:2101.06820.

Fister, I., Yang, X. S., & Brest, J. (2014). On the randomized firefly algorithm. In *Cuckoo search and firefly algorithm* (pp. 27–48). Springer. doi:10.1007/978-3-319-02141-6_2

Gálvez, J., Cuevas, E., Becerra, H., & Avalos, O. (2019). A hybrid optimization approach based on clustering and chaotic sequences. *International Journal of Machine Learning and Cybernetics*, *11*(2), 359–401. doi:10.1007/s13042-019-00979-6

Gandomi, A., Yang, X., Talatahari, S., & Alavi, A. (2013). Firefly algorithm with chaos. *Communications in Nonlinear Science and Numerical Simulation*, *18*(1), 89–98. doi:10.1016/j.cnsns.2012.06.009

Gharooni-fard, G., Moein-darbari, F., Deldari, H., & Morvaridi, A. (2010). Scheduling of scientific workflows using a chaos-genetic algorithm. *Procedia Computer Science*, *1*(1), 1445–1454. doi:10.1016/j.procs.2010.04.160

Giri, P. K., De, S. S., Dehuri, S., & Cho, S. B. (2017). Locally and globally tuned chaotic biogeography-based optimization algorithm. In *2017 International Conference on Information Technology (ICIT)* (pp. 152-158). IEEE. doi:10.1109/ICIT.2017.44

Goel, S. (2011). Generation of New Fractal Models and Study of Stability of Iterative Procedures (Ph.D). Gautam Buddh Technical University, Lucknow, India.

Guo-ping, Y., San-yang, L., Jian-ke, Z., & Hai-lin, F. (2016). Parameter estimation for discrete chaotic systems with biogeography-based optimization. *Journal of Lanzhou University: Natural Sciences*, *52*(6), 832–837.

Han, Y., Ding, J., Du, L., & Lei, Y. (2021). *Control and anti-control of chaos based on the moving largest Lyapunov exponent using reinforcement learning*. 10.21203/rs.3.rs-176868/v1

Heidari, A., Mirvahabi, S., & Homayouni, S. (2015). An effective hybrid support vector regression with chaos-embedded biogeography-based optimization strategy for prediction of earthquake-triggered slope deformations. *The International Archives of the Photogrammetry, Remote Sensing and Spatial Information Sciences*, *XL-1*(W5), 301–305. doi:10.5194/isprsarchives-XL-1-W5-301-2015

Jalili, S., Hosseinzadeh, Y., & Kaveh, A. (2014). Chaotic biogeography algorithm for size and shape optimization of truss structures with frequency constraints. *Periodica Polytechnica. Civil Engineering*, *58*(4), 397–422. doi:10.3311/PPci.7466

Jin, Q., Lin, N., & Zhang, Y. (2021). K-means clustering algorithm based on chaotic adaptive artificial bee colony. Algorithms, 14(2), 53.

Kaur, A., Pal, S. K., & Singh, A. P. (2020). Hybridization of chaos and flower pollination algorithm over K-means for data clustering. *Applied Soft Computing*, *97*, 105523. doi:10.1016/j.asoc.2019.105523

Khanna, M., Chaudhary, A., Toofani, A., & Pawar, A. (2019). Performance comparison of multi-objective algorithms for test case prioritization during web application testing. *Arabian Journal for Science and Engineering*, *44*(11), 9599–9625. doi:10.1007/s13369-019-03817-7

Khanna, M., Chauhan, N., & Sharma, D. K. (2019). Search for prioritized test cases during web application testing. *International Journal of Applied Metaheuristic Computing*, *10*(2), 1–26. doi:10.4018/IJAMC.2019040101

Krasnosel'skiı, M. A. (1955). Two remarks on the method of successive approximations. *Uspekhi Matematicheskhi Nauk*, *10*, 123–127.

Lesmoir-Gordon, N., & Rood, W. (2014). *Introducing fractals: A graphic guide*. Icon Books Ltd.

Levinsohn, E. A., Mendoza, S. A., & Peacock-López, E. (2012). Switching induced complex dynamics in an extended logistic map. *Chaos, Solitons, and Fractals*, *45*(4), 426–432. doi:10.1016/j.chaos.2011.12.020

Li-Jiang, Y., & Tian-Lun, C. (2002). Application of chaos in genetic algorithms. *Communications in Theoretical Physics*, *38*(2), 168–172. doi:10.1088/0253-6102/38/2/168

Linglong, T., Yehui, C., & Changkai, L. (2018). Research on image segmentation optimization algorithm based on chaotic particle swarm optimization and fuzzy clustering. In *Proceedings of the 2018 7th International Conference on Software and Computer Applications* (pp. 178-182). doi:10.1145/3185089.3185139

Liu, B., Wang, L., Jin, Y. H., Tang, F., & Huang, D. X. (2005). Improved particle swarm optimization combined with chaos. *Chaos, Solitons, and Fractals*, *25*(5), 1261–1271. doi:10.1016/j.chaos.2004.11.095

Lu, X., Wu, Q., Zhou, Y., Ma, Y., Song, C., & Ma, C. (2019). A dynamic swarm firefly algorithm based on chaos theory and max-min distance algorithm. *Traitement du Signal*, *36*(3), 227–231. doi:10.18280/ts.360304

Ma, H., Simon, D., Siarry, P., Yang, Z., & Fei, M. (2017). Biogeography-based optimization: A 10-year review. *IEEE Transactions on Emerging Topics in Computational Intelligence*, *1*(5), 391–407. doi:10.1109/TETCI.2017.2739124

MacArthur, R. H. (2010). *The Theory of Island Biogeography Revisited* (J. B. Losos & R. E. Ricklefs, Eds.). Princeton University Press.

Maier, M. P., & Peacock-López, E. (2010). Switching induced oscillations in the logistic map. *Physics Letters. [Part A]*, *374*(8), 1028–1032. doi:10.1016/j.physleta.2009.12.039

Mann, W. R. (1953). Mean value methods in iteration. *Proceedings of the American Mathematical Society*, *4*(3), 506–510. doi:10.1090/S0002-9939-1953-0054846-3

Mendoza, S. A., Matt, E. W., Guimarães-Blandón, D. R., & Peacock-López, E. (2018). Parrondo's paradox or chaos control in discrete two-dimensional dynamic systems. *Chaos, Solitons, and Fractals*, *106*, 86–93. doi:10.1016/j.chaos.2017.11.011

Mingjun, J., & Huanwen, T. (2004). Application of chaos in simulated annealing. *Chaos, Solitons, and Fractals*, *21*(4), 933–941. doi:10.1016/j.chaos.2003.12.032

Negi, A. & Rani, M. (2008a). A new approach to dynamic noise on superior Mandelbrot set. *Chaos, Solitons & Fractals, 36*(4), 1089-1096.

Negi, A. & Rani, M. (2008b). Midgets of superior Mandelbrot set. *Chaos, Solitons & Fractals, 36*(2), 237-245.

Negi, A., Rani, M., & Mahanti, P. K. (2008). Computer simulation of the behaviour of Julia sets using switching processes. *Chaos, Solitons & Fractals, 37*(4), 1187-1192.

Peacock-López, E. (2011). Seasonality as a Parrondian game. *Physics Letters. [Part A]*, *375*(35), 3124–3129. doi:10.1016/j.physleta.2011.06.063

Pecora, L. M., & Carroll, T. L. (1990). Synchronization in chaotic systems. *Physical Review Letters*, *64*(8), 821–825. doi:10.1103/PhysRevLett.64.821 PMID:10042089

Rani, M., & Agarwal, R. (2009). A new experimental approach to study the stability of logistic map. *Chaos, Solitons, and Fractals*, *41*(4), 2062–2066. doi:10.1016/j.chaos.2008.08.022

Rani, M., & Yadav, A. (2016). Parrondo's paradox in the superior logistic map. *Int. J Tech. Res*, *1*(2), 1–8.

Saremi, S., & Mirjalili, S. (2013). Integrating chaos to biogeography-based optimization algorithm. *International Journal of Computer and Communication Engineering*, *2*(6), 655–658. doi:10.7763/IJCCE.2013.V2.268

Saremi, S., Mirjalili, S., & Lewis, A. (2014). Biogeography-based optimisation with chaos. *Neural Computing & Applications*, *25*(5), 1077–1097. doi:10.1007/s00521-014-1597-x

Simon, D. (2008). Biogeography-based optimization. *IEEE Transactions on Evolutionary Computation*, *12*(6), 702–713. doi:10.1109/TEVC.2008.919004

Simon, D. (2011). A probabilistic analysis of a simplified biogeography-based optimization algorithm. *Evolutionary Computation*, *19*(2), 167–188. doi:10.1162/EVCO_a_00018 PMID:20807078

Singh, L. K., Garg, H., & Khanna, M. (2021). An artificial intelligence-based smart system for early glaucoma recognition using OCT images. *International Journal of E-Health and Medical Communications*, *12*(4), 32–59. doi:10.4018/IJEHMC.20210701.oa3

Singh, L. K., Khanna, M., & Garg, H. (2020). Multimodal biometric based on fusion of ridge features with minutiae features and face features. *International Journal of Information System Modeling and Design*, *11*(1), 37–57. doi:10.4018/IJISMD.2020010103

Singh, S. L., Mishra, S. N., & Sinkala, W. (2012). A new iterative approach to fractal models. *Communications in Nonlinear Science and Numerical Simulation*, *17*(2), 521–529. doi:10.1016/j.cnsns.2011.06.014

Singh, T. (2020). A chaotic sequence-guided Harris hawks optimizer for data clustering. *Neural Computing & Applications*, *32*(23), 17789–17803. doi:10.1007/s00521-020-04951-2

Strogatz, S. H. (2018). *Nonlinear dynamics and chaos with student solutions manual: With applications to physics, biology, chemistry, and engineering*. CRC Press. doi:10.1201/9780429399640

Talatahari, S., Azar, B. F., Sheikholeslami, R., & Gandomi, A. H. (2012). Imperialist competitive algorithm combined with chaos for global optimization. *Communications in Nonlinear Science and Numerical Simulation*, *17*(3), 1312–1319. doi:10.1016/j.cnsns.2011.08.021

Thawkar, S., Singh, L. K., & Khanna, M. (2021). Multi-objective techniques for feature selection and classification in digital mammography. *Intelligent Decision Technologies*, *15*(1), 115–125. doi:10.3233/IDT-200049

Wallace, A. (2005). *The geographical distribution of animals (two volumes)*. Adamant Media Corporation.

Wang, G. G., Guo, L., Gandomi, A. H., Hao, G. S., & Wang, H. (2014). Chaotic Krill Herd algorithm. *Information Sciences*, *274*, 17–34. doi:10.1016/j.ins.2014.02.123

Wang, J. S., & Song, J. D. (2017). Chaotic biogeography-based optimization algorithm. *IAENG International Journal of Computer Science*, *44*(2), 122–134.

Wang, L., Liu, X., Sun, M., Qu, J., & Wei, Y. (2018). A new chaotic starling particle swarm optimization algorithm for clustering problems. *Mathematical Problems in Engineering*, *2018*, 2018. doi:10.1155/2018/8250480

Wang, S. H., Lu, H. M., Li, Y. J., Wang, Y., Chen, Z. M., Wei, Y. M., & Zhang, Y. D. (2016). A new logistic map based chaotic biogeography-based optimization approach for cluster analysis. In *2016 International Conference on Progress in Informatics and Computing (PIC)* (pp. 88-92). IEEE. doi:10.1109/PIC.2016.7949472

Wilcoxon, F. (1992). Individual comparisons by ranking methods. In *Breakthroughs in Statistics* (pp. 196–202). Springer. doi:10.1007/978-1-4612-4380-9_16

Yadav, A., & Rani, M. (2015). Modified and extended logistic map in superior orbit. *Procedia Computer Science*, *57*, 581–586. doi:10.1016/j.procs.2015.07.397

Yakubu, H. J., & Aboiyar, T. (2018). A chaos-based image encryption algorithm using Shimizu-Morioka system. *International Journal of Communication and Computer Technologies*, *6*(1), 7–11.

Yang, D., Li, G., & Cheng, G. (2007). On the efficiency of chaos optimization algorithms for global optimization. *Chaos, Solitons, and Fractals*, *34*(4), 1366–1375. doi:10.1016/j.chaos.2006.04.057

Zhu, X., Luo, W., & Zhu, T. (2014). An improved genetic algorithm for dynamic shortest path problems. In *2014 IEEE Congress on Evolutionary Computation (CEC)* (pp. 2093-2100). IEEE. doi:10.1109/CEC.2014.6900496

Zhu, Z., Liu, Y., & Wang, Y. (2020). Noise robust hybrid algorithm for segmenting image with unequal cluster sizes based on chaotic crow search and improved fuzzy c-means. *Journal of Intelligent & Fuzzy Systems*, *39*(5), 7005–7020. doi:10.3233/JIFS-200197

Deepak Kumar is a research scholar in the department of computer science and has interests in computational intelligence, nature inspired algorithms, fractals and chaos, data mining etc. Mamta Rani is an associate professor and HOD in Dept. of Computer Science in the Central University of Rajasthan, Kishangarh, Rajasthan.